Copy 259
RM E51I04

NACA

RESEARCH MEMORANDUM

INVESTIGATION OF THE LIQUID FLUORINE - LIQUID

DIBORANE PROPELLANT COMBINATION IN A

100-POUND-THRUST ROCKET ENGINE

By Paul M. Ordin, Howard W. Douglass
and William H. Rowe

Lewis Flight Propulsion Laboratory
Cleveland, Ohio

NATIONAL ADVISORY COMMITTEE
FOR AERONAUTICS
WASHINGTON
November 30, 1951

3, 9, 98/13

NATIONAL ADVISORY COMMITTEE FOR AERONAUTICS

RESEARCH MEMORANDUM

INVESTIGATION OF THE LIQUID FLUORINE - LIQUID DIBORANE

PROPELLANT COMBINATION IN A 100-POUND-THRUST

ROCKET ENGINE

By Paul M. Ordin, Howard W. Douglass, and William H. Rowe

SUMMARY

Specific impulse, volume specific impulse, characteristic velocity, thrust coefficient, and heat rejection of liquid fluorine and liquid diborane for a range of mixture ratio were determined in a 100-pound-thrust rocket engine designed for a combustion-chamber pressure of 300 pounds per square inch absolute.

In engines with a characteristic length L^* (volume/throat area) of 100 inches, the maximum experimental specific impulse obtained was 280 pound-seconds per pound at 14 weight percent of fuel; the correction for the heat rejection (5.28 Btu/(sec)(sq in.)) and for deviations from the reference combustion-chamber pressure raised this value to 286 pound-seconds per pound. The maximum volume specific impulse was 326X62.4 pound-seconds per cubic foot at 11 weight percent of fuel. The characteristic velocity reached a maximum of 6400 feet per second and the experimental thrust coefficient averaged 1.33.

The theoretical performance was recalculated with revised thermodynamic data, indicating a maximum specific impulse of 311 pound-seconds per pound as compared with the previously reported value of 323.

Considerable difficulty was experienced in developing a suitable injector; it was necessary to employ a protective sheath of helium around the diborane injection hole to prevent injector burnout. The results obtained with the various engines indicated lower performance with the 50 L^* than with the 100 L^* engines using the same injector and comparable amounts of protective helium. Decreasing the quantity of helium or increasing the L^* of the engine resulted in higher performance.

Methods of handling and transporting liquid fluorine in a trailer and techniques in condensing gaseous fluorine from commercial supply cylinders were developed.

INTRODUCTION

The best oxidizers for long-range rocket-powered vehicles are liquid fluorine and liquid ozone, as established by calculations in which high specific impulse and bulk density are prime factors. Two comparisons (references 1 and 2) indicate fluorine is superior, although a third (reference 3) favors ozone.

Maximum theoretical specific impulse values, based on equilibrium expansion from a combustion-chamber pressure of 300 pounds per square inch absolute, for fluorine with various fuels are tabulated as follows:

Fuel	Specific impulse (lb-sec/lb)	Reference
Hydrogen H_2	341	4
Lithium Li	335	5
Diborane B_2H_6	323	6
Hydrazine N_2H_4	315	(a)
Ammonia NH_3	311	4

[a]Unpublished NACA data.

Boron hydrides have been considered as rocket fuels because of their high heats of combustion. The theoretical performance of diborane with several oxidizers is given by reference 6; experimental performance of diborane with hydrogen peroxide and liquid oxygen is presented in references 7 and 8. As an extension of this study, diborane was selected as the initial fuel to be investigated with fluorine.

The experimental investigation of diborane and fluorine was conducted at the NACA Lewis laboratory using a 100-pound-thrust rocket engine at a combustion-chamber pressure of 300 pounds per square inch absolute. Experimental values were determined for specific impulse, volume specific impulse, characteristic velocity, thrust coefficient, and heat rejection for a range of propellant mixture ratio. In addition, effects of variations of propellant injection methods and characteristic engine lengths L^* on the performance were observed. Methods of handling and transporting fluorine were developed and a revised theoretical performance curve was obtained from calculations based on new thermochemical data.

2293

PROPELLANTS AND APPARATUS

Propellants and Handling Systems

Physical constants of fluorine and diborane are given in table I. Diborane was obtained by the NACA through the cooperation of the Bureau of Aeronautics, Department of the Navy. Impurities amounted to approximately 1 percent of ethane in the diborane.

Fluorine of at least 98-percent purity was obtained from two sources; commercial gas cylinders and direct condensation from fluorine cells into a trailer. Fluorine obtained from a local supplier was passed from the electrolytic cell through an electric furnace (300° C) to remove any oxygen bifluoride present. The fluorine was next passed through two successive sodium fluoride pill towers (100° and -40° C) to remove hydrogen fluoride and then into a condensing unit in a trailer.

A sketch of the trailer fitted with a condensing system to receive, liquify, and transport a maximum of 12 pounds of fluorine is shown in figure 1. The fluorine tank and vacuum-jacketed liquid-nitrogen bath assembly were suspended from a balance beam and enclosed in a protective steel cylinder (fig. 2). The tank assembly was raised by a pneumatic lift while in travel to prevent damage of the balance equipment. During a firing the balance beam transmitted the change in weight of the fluorine tank to a strain gage spring, the output of which was recorded by a self-balancing potentiometer.

During the latter part of the program, the condensing system was permanently mounted at the laboratory, permitting liquification from commercial supply cylinders. The fluorine tank alone, completely immersed and buoyed by a constant-level liquid-nitrogen bath, was suspended directly from a cantilever strain-gage beam, providing more sensitive flow-rate measurements during rocket firing.

A diagrammatic sketch of the complete flow system is shown in figure 3. Facilities were provided for cooling propellant lines and valves with dry ice or liquid nitrogen; in addition, the fluorine lines and part of the diborane lines were vacuum-jacketed. Charcoal-purified helium controlled by two-stage pressure regulation was used to force the propellants into the combustion chamber. For the oxidant system, the pressurizing helium was precooled by liquid nitrogen to prevent vaporization of the fluorine. Packless-type valves, either hand operated or remote operated, were used in the oxidant system. Photographs of the fluorine system and the thrust stand are shown in figures 4 and 5.

Engine Assembly

The engine assembly was comprised of two units, a combustion chamber with nozzle and a propellant injector, both fabricated from "Z"-nickel. The engines were designed for a thrust of 100 pounds, a combustion-chamber pressure of 300 pounds per square inch absolute, and characteristic lengths L^* of 50, 89, and 100 inches.

The combustion chamber and nozzle were cooled by means of water flow through a 0.050-inch annular coolant passage. Three longitudinal copper fins, spaced 120° apart, were silver-soldered to the inner shell to provide uniform coolant distribution. Figure 6 is a photograph of a section through the engine. A water flow of approximately 10 pounds per second from a pressurized supply tank provided sufficient capacity to cool the engine. This flow corresponds to a velocity of about 190 feet per second through the annulus at the critical throat section of the nozzle. Figure 7 is a dimensional drawing of the combustion chamber and nozzle used for most of the investigation.

The types of injector used for the investigation included a modified multiple impinging jet (fig. 8), a hollow-cone spray type (fig. 9), a shower head (fig. 10), a four fluorine - one diborane impinging-jet type employing a helium sheath around the diborane entrance (fig. 11), and a four unit two fluorine - one diborane impinging-jet injector employing a helium sheath around each diborane inlet (fig. 12).

INSTRUMENTATION

Propellant flows were measured by strain gages cemented on cantilever beams. These strain-gage elements were connected by resistance-bridge circuits to continuous-recording self-balancing potentiometers. Matching units in each circuit provided adjustable ranges of 1, 2, and 4 pounds for the diborane system, and 5, 10, and 20 pounds for the fluorine system for full-scale chart readings. The wiring circuit was based on principles presented in reference 9.

Dead-weight calibrations of the weighing systems were made before and after each run; the over-all variation for the fluorine system during the investigation was less than 0.6 percent and for the diborane system, less than 0.4 percent. The precision of the flow measurements for the fluorine system was within 2 percent and for the diborane, 1 percent. When the fluorine system was modified to reduce the load friction, the precision was within 1 percent.

The engine thrust was also measured by means of a strain-gage system. The full-scale range could be adjusted for 50, 100, or 200 pounds thrust. Dead-weight calibrations made before and after runs agreed within 1 percent; calibrations during the entire investigation varied less than 2 percent. The precision of the thrust measurement was within 2.5 percent.

Combustion-chamber pressure was measured by a Bourdon-tube pressure recorder located within a few feet of the engine. Propellant tank pressures and combustion-chamber pressure in addition to being observed remotely by means of Bourdon gages were recorded by a modified aerial camera.

The engine cooling-water flow was measured by an adjustable orifice equipped with an electric transmitter and recorder. The accuracy of the water-flow measurement was within 2 percent.

A critical-flow orifice was used to control the flow of helium protecting the diborane jets.

Copper-constantan thermocouples were used to measure engine coolant-water temperature rise and were also placed in the oxidant flow line to determine the extent of precooling. All temperatures were recorded on self-balancing continuous-recording potentiometers within an accuracy of 1 percent.

PROCEDURE

All lines and valves were pressure checked and flushed with helium gas prior to loading of propellants. Diborane was transferred from dry-ice storage to the propellant tank, which was maintained in a dry-ice - alcohol bath until the run. Then fluorine was condensed into the oxidant tank (or, before the modification, the pressurizing and flow lines of the loaded trailer were connected to the system).

The firing procedure was conducted from the remote-control room: A flow of liquid nitrogen was passed through the fluorine flow line until the system reached liquid-nitrogen temperature; the nitrogen was shut off and the fluorine flow begun; approximately 1 second later the diborane was injected, producing immediate ignition. After each run (5 to 20 sec in length) the systems were purged and a helium atmosphere was maintained in the propellant tanks.

With the comparatively large characteristic-length engines used, a significant amount of heat was lost to the engine walls. The loss was determined by the product of the temperature rise of the coolant water, the specific heat of water, and the water-flow rate. The experimental specific impulse values were corrected for this heat loss to the engine walls in terms of the theoretical thermodynamic efficiency and the total measured heat rejection as represented in the expression:

$$I_{corr} = \sqrt{I^2_{exp} + \frac{2J}{g} Q\eta}$$

where

I_{corr} experimental specific impulse corrected for heat rejection (lb-sec/lb)

I_{exp} experimental specific impulse, measured (lb-sec/lb)

J mechanical equivalent of heat (778 ft-lb/Btu)

g gravitational constant (32.17 ft/sec^2)

Q heat rejection per propellant weight (Btu/lb)

η ideal thermal cycle efficiency $\left(1 - \dfrac{T_e}{T_c}\right)$

T_e theoretical exit temperature (°K)

T_c theoretical combustion-chamber temperature (°K)

A further correction consisted in adjusting the experimental performance to a pressure basis of 300 pounds per square inch absolute. Pressure corrections were generally very small and were determined from the following expression:

$$\Delta I_p = K(\log P_1 - \log P_2)$$

where

ΔI_p change in specific impulse due to pressure difference

K rate of change of specific impulse with log of combustion-chamber pressure, estimated to be 66.9 from theoretical data on $H_2\text{-}F_2$ and $NH_3\text{-}F_2$ presented in reference 4

P_1 desired combustion-chamber pressure (300 lb/sq in. absolute)

P_2 experimental combustion-chamber pressure (lb/sq in. absolute)

The pressure correction ΔI_p was combined with the experimentally measured value corrected for heat rejection to enable comparison with the theoretical performance.

In calculating the experimental specific impulse obtained during a run in which helium was used as a protective sheath, the helium was included in the total flow of propellants. In addition, one calculation was made to determine the effect of the addition of 4 percent of helium on the theoretical performance of the liquid fluorine - liquid diborane propellant combination.

Values of characteristic velocity and thrust coefficient were obtained from the results of the experimental data using the equations

$$c^* = \frac{P_c A_t \, g}{w}$$

and

$$C_F = \frac{T}{P_c A_t}$$

where

c^* characteristic velocity (ft/sec)

P_c combustion chamber pressure (lb/sq in. absolute)

A_t exhaust-nozzle throat area (sq in.)

g gravitational constant (32.17 ft/sec^2)

w total propellant flow (lb/sec)

C_F thrust coefficient

T thrust (lb)

RESULTS

Theoretical Performance

The theoretical performance of the diborane-fluorine propellant combination was recalculated from reference 6 using the following revised thermodynamic data: a change of the heat of formation of diborane from -44 to 7.5 kcal per mole (reference 10); a change of the heat of dissociation of fluorine from 63.5 to 35.6 kcal per mole (reference 10); and newly calculated thermodynamic data for hydrogen fluoride (reference 10). The results are shown by figure 13 where specific impulse, combustion-chamber temperature, and exit temperature for liquid fluorine and diborane are presented as a function of the ratio of fuel weight to total propellant weight. Included in figure 13 are theoretical curves obtained from reference 6. The new theoretical curve indicates a maximum specific impulse of 311 pound-seconds per pound as compared with the previously reported value of 323 pound-seconds per pound. All curves are based on equilibrium expansion through an ideal nozzle, using propellants of 100-percent purity.

Experimental Performance

Specific impulse. - The experimental specific impulse is shown by figure 14(a) for a propellant mixture range of 7 to 31 weight percent fuel; the theoretical (ideal) curve is also shown for comparison. A compilation of the experimental data is given in table II. The curve, drawn through the experimental points obtained with the 100 L^* engine (solid line), follows the theoretical curve within 88 percent in the region of 10 to 19 weight percent fuel. A maximum experimental value of 280 pound-seconds per pound was obtained at 14 weight percent fuel, compared with the theoretical maximum of 311 at 15 weight percent fuel. The stoichiometric ratio is 10.8 percent.

The performance obtained with a 50 L^* engine and a helium-protected injector was lower in the range of maximum performance than that of a 100 L^* engine. Decreasing the quantity of helium used in the 50 L^* engine brought its performance closer to the 100 L^* values. In the fuel-lean (5 to 9 weight percent fuel) and fuel-rich (20 to 30 weight percent fuel) regions, where only 50 L^* engines were used, extremely low performance was obtained (dashed extension curves). Injector types used with the 100 L^* engines were the four-one hollow-cone spray, the four-one solid jet with helium, and the four set, two-one solid jet with helium. For the 50 L^* engines, the shower-head injector, the modified impinging jet, and the four-one solid jet with helium were used.

The theoretical curve, adjusted for nonparallel flow, and the experimental curve, corrected for deviation from the desired combustion-chamber pressure of 300 pounds per square inch absolute and for heat

rejection to the engine walls, are shown in figure 14(b). This theoretical curve is approximately 2 percent lower than the ideal one because of the 30° divergent angle of the exhaust nozzle; it indicates a maximum specific impulse of 306 pound-seconds per pound. The experimental curve is raised approximately 2 percent by its correction to a maximum specific impulse of 286 pound-seconds per pound. Included in figure 14(b) is a theoretically calculated point (ideal) in which the protective helium was considered as a working fluid in the rocket engine. Although the addition of helium (4 percent of total propellant) indicated a drop in combustion-chamber temperature of approximately 160° K, a more significant drop in average molecular weight resulted in an approximate 3-percent increase in theoretical specific impulse from 311 to 320 pound-seconds per pound. In units employing helium-pressurized propellant tanks, addition to the combustion chamber of a small percentage of this helium as a working fluid may be worthy of further consideration as a means of providing booster performance.

Characteristic velocity and nozzle coefficient. - A comparison of the theoretical and experimental characteristic-velocity C^* curves is presented in figure 15. The theoretical values were obtained using the ratio of specific heats γ for combustion-chamber conditions. The C^* curve drawn through the experimental points obtained with the 100 L^* engine (solid line) follows the theoretical curve within 94 percent in the region of 9 to 18 weight percent fuel. The maximum experimental C^* value is 6400 feet per second (94 percent of theoretical) at 15 weight percent fuel.

A plot of the thrust coefficient values C_F against propellant mixture ratio is also shown in figure 15. Because considerable scatter was obtained in the experimental data, a line was drawn representing the arithmetic average. This average value was 1.33 as compared with the calculated value of 1.37.

Heat rejection. - The measured engine heat rejection is presented in figure 15 as a function of the ratio of fuel weight to total propellant weight. The measured heat release parallels performance, with a maximum of 272 Btu per second (5.28 Btu/(sec)(sq in.) for a 100 L^* engine) at 15 weight percent fuel.

Volume specific impulse. - Volume specific impulse is plotted against the ratio of fuel weight to total propellant weight in figure 16(a). The experimental curve drawn through the points obtained with the 100 L^* engine (solid line) shows a maximum of 326X62.4 pound-seconds per cubic foot at 11 percent fuel (volume of helium neglected); the theoretical maximum is 373X62.4 pound seconds per cubic foot at 10 percent fuel. In computing these data, the density of fluorine was taken as 1.56 grams per cubic centimeter instead of the literature value of 1.108. The higher density was based on unpublished information obtained from Aerojet Engineering Corp. (Azusa, California) and on

recent experiences of the NACA. A plot of the actual flow rates of
liquid fluorine and liquid nitrogen for the same injector is included
in figure 16(b). Assuming the orifice flow coefficients to be the same
for the two liquids and using a density of 0.808 gram per cubic centi-
meter for liquid nitrogen results in a fluorine density of 1.6 grams
per cubic centimeter. This value compares favorably with the value of
1.558 grams per cubic centimeter obtained by the Aerojet Engineering
Corp.

DISCUSSION

Considerable difficulty was experienced in obtaining a satisfactory
injector for the fluorine-diborane combination. The modified multiple
impinging jet and the hollow-cone spray injectors (figs. 8 and 9) both
burned at the injector face where the diborane holes were located.
Three runs were made with the multiple impinging-jet injector at differ-
ent fuel-oxidant ratios and under different injection conditions of fuel
first and oxidant first, but in each case the injector burned. A photo-
graph of the injector indicating the burned area around the diborane
inlet is shown in figure 17. With the shower-head injector (fig. 10),
all the diborane holes welded completely shut, stopping the flow of
fuel. A photograph of the shower-head injector after the run is shown
in figure 18.

Since in all the runs made with these injectors the diborane holes
were either burned or welded, it became apparent that the flame speed of
diborane with fluorine was sufficiently high to cause the flame to seat
directly at the injector face. Recent experiments (reference 11) have
shown that mixtures containing 10 percent or more of diborane with
oxygen invariably detonate. The detonation velocities are 6000 to
7000 feet per second and, in all likelihood, are greater for diborane
with fluorine.

In order to prevent the flame from seating at the injector face, a
protective sheath of helium was provided for the diborane jet in a four
fluorine - one diborane impinging-jet design (fig. 11). A 0.020-inch
annulus supplied the helium around a center jet of diborane, and
four jets of fluorine impinged on the diborane at a 30° angle, $1\frac{1}{8}$ inches

from the injector face (fig. 19). This injector proved successful
since no further injector burnouts were experienced.

An injector to provide better propellant mixing than that given by
the four-one design, while still utilizing helium protection for the
diborane jets, was fabricated with four sets of holes for two fluorine -
one diborane impingement (fig. 12). The one run made with this injector
yielded results no better than those obtained with the four fluorine -
one diborane injector.

2293

The results of the investigation (in the region of 10 to 19 weight
percent fuel), indicate that the use of the helium sheath required some-
what larger combustion-chamber volume requirements to obtain complete
combustion before expansion. The increase in performance resulting from
a decrease in helium flow in the 50 L^* engine points to the possibility
of a transient mixing and burning zone dependent on the helium-flow
rate; the lower the helium-flow rate the closer the burning zone is
allowed to approach the injector face and the greater the effective
combustion-chamber volume available for reaction.

The reasons for the low performance obtained in the fuel-lean and
fuel-rich regions, in which only 50 L^* engines were used, are unknown
and would require further investigation. The low performance may be
attributed to factors affected by low combustion-chamber pressure (mix-
ing, reaction rates, and expansion ratio). The possibility also exists
that a variety of injection patterns is required to cover a wide fuel-
oxidant range with maximum efficiency. This conjecture is made because
of the extremely low performance obtained in the fuel-lean region with
the four-one injector using a low helium flow and the high performance
obtained with the same engine and injector in the region at 17 weight
percent fuel. Similar results are evident in the plot of characteristic
velocity C^* against weight percent fuel.

Considerable variation occurred in the values for thrust coeffi-
cient C_F. The reasons for the scatter are unknown but may indicate a
variable thrust constant due to the dynamics of the flow systems or
point to the possibility of a reaction taking place during expansion
through the nozzle resulting in a ratio of specific heats far different
from that based on ideal conditions.

Although injectors employing protective sheaths of helium proved
successful in preventing injector failures, a great deal of difficulty
was experienced in the form of engine burnouts. Examination of the
injector and combustion chamber after running indicated burning of the
engine flange junction and, in many cases, after the second or third run
with the same engine, a complete burning through at the convergent sec-
tion of the exhaust nozzle. The burned area at the flange appeared to
have a definite pattern; a photograph of a typical burn is presented in
figure 20. The configuration appears to indicate a reversal of flow of
the hot gases from the center of the combustion chamber back along the
uncooled inside surfaces of the flanges to the injector and then down-
stream again. The engine failures at the convergent section may have
been due to an unequal distribution of the cooling water through the
annulus or by repeated impact of molten metal from the burned flange.

During part of the investigation the toxic exhaust gases were
introduced into a water scrubber consisting of a 12-inch duct, 5 feet
long. Approximately 4 pounds per second of water were introduced through

three perforated copper rings in an effort to absorb and remove the
toxic gases in a water stream. Because of the limited supply of water,
the scrubber was not completely effective since the absorbed gases
issued in a cloud of steam. After a number of runs, the scrubber was
destroyed by an explosion. Data obtained for propellant flows and
thrust indicate that the explosion occurred about 1 second after the
beginning of the run. Since the helium protected diborane was injected
first for this run, some quantity of unburned diborane may have entered
the scrubber and reacted with the water evolving hydrogen. The explo-
sion could then have been caused by ignition of the hydrogen by the
rocket exhaust flame.

SUMMARY OF RESULTS

The theoretical performance of the liquid fluorine - liquid
diborane propellant combination was recalculated with revised data, and
experiments were conducted to determine the performance in a 100-pound-
thrust rocket engine at a combustion-chamber pressure of 300 pounds per
square inch absolute. The investigation produced the following results:

1. The revised theoretical performance calculations for equilibrium
expansion indicated a maximum specific impulse of 311 pound-seconds per
pound, as compared with the previously calculated maximum of 323.

2. The use of normally accepted injector designs (impinging jet,
shower head, and spray type) resulted in injector burnouts; a satis-
factory solution involved the use of a protective sheath of helium
around the diborane jets.

3. Theoretical and experimental performance curves reached a maxi-
mum near a ratio of fuel weight to total propellant weight of 0.15. The
maximum experimental specific impulse was 280 pound-seconds per pound,
approximately 88 percent of the ideal theoretical value.

4. The maximum specific impulse increased to approximately
286 pound-seconds per pound when corrected for heat loss and small
deviations of combustion-chamber pressure from 300 pounds per square
inch absolute. This value is 93 percent of the theoretical specific
impulse for nozzle used.

5. In the region of maximum performance, runs made with an engine
having a characteristic length L^* of 50 inches and the four fluorine -
one diborane helium-sheathed injector resulted in lower performance
than when comparable amounts of helium were used in the 100 L^* engine
tests. Decreasing the quantity of helium resulted in an increase in
performance, approaching the values obtained in the 100 L^* engine.

6. One calculation made to obtain the theoretical performance using 4 percent helium as a diluent resulted in an increased specific impulse for equilibrium composition from 311 to 320 pound-seconds per pound.

7. The experimental characteristic velocity reached a maximum of 6400 feet per second at 15 weight percent fuel; this is 94 percent of the calculated theoretical maximum.

8. The experimental thrust coefficient averaged 1.33 as compared with the theoretical value of 1.37.

9. The heat rejection to the walls was high, causing a considerable number of engine burnouts. The maximum heat rejection of approximately 5.28 Btu per second per square inch for the 100 L^* engine occurred in the region of maximum performance.

10. The maximum experimental volume specific impulse was 326X62.4 pound-seconds per cubic foot and occurred at 11 weight percent fuel; this value was obtained by using a density of fluorine of approximately 1.56 grams per cubic centimeter.

Lewis Flight Propulsion Laboratory
    National Advisory Committee for Aeronautics
        Cleveland, Ohio

REFERENCES

1. Myers, T. E., Friedman, J., and Kanarek, I. A.: Comparison and Evaluation of Rocket Motor Propellant Combination. Rep. No. AL-998, Proj. MX-770, North American Aviation, Inc., Feb. 7, 1950.

2. Canright, R. B.: The Relative Importance of Specific Impulse and Propellant Density for Large Rockets. Rep. No. 4-29, Jet Prop. Lab., C.I.T., Jan. 7, 1947. (Ordcit Proj. Contract No. W-04-200-ORD-455.)

3. Gordon, Robert: The Relative Importance of Propellant Density and Specific Impulse on Satellite Vehicle Performance. Rep. No. R-92, May 5, 1948. (Amendment 1, Item 4, Bur. Aero. Contract NOa(s)-8496.)

4. Morrell, Virginia E.: Effect of Combustion-Chamber Pressure and Nozzle Expansion Ratio on Theoretical Performance of Several Rocket Propellant Systems. NACA RM E50C30, 1950.

5. Gordon, Sanford, and Huff, Vearl N.: Theoretical Performance of Lithium and Fluorine as a Rocket Propellant. NACA RM E51C01, 1951.

6. Huff, Vearl N., Calvert, Clyde S., and Erdmann, Virginia C.: Theoretical Performance of Diborane as a Rocket Fuel. NACA RM E8I17a, 1949.

7. Rowe, William H., Ordin, Paul M., and Diehl, John M.: Investigation of the Diborane-Hydrogen Perioxide Propellant Combination. NACA RM E7K07, 1948.

8. Rowe, William H., Ordin, Paul M., and Diehl, John M.: Experimental Investigation of Liquid Diborane - Liquid Oxygen Propellant Combination in 100-Pound-Thrust Rocket Engine. NACA RM E9C11, 1949.

9. Warshawsky, Isidore: A Multiple Bridge for Elimination of Contact-Resistance Errors in Resistance Strain-Gage Measurements. NACA TN 1031, 1946.

10. Huff, Vearl N., and Gordon, Sanford: Table of Thermodynamic Functions for Analysis of Aircraft-Propulsion Systems. NACA TN 2161, 1950.

11. Price, F. P.: Burning and Detonation of Mixtures of Boron Hydrides with Air and Oxygen. Rep. No. R50A0504, Apparatus Dept., Gen. Elec. Co., March 1950. (Proj. Hermes, Ord. Dept.)

12. Doyle, W. L.: Preliminary Evaluation of Liquid Fluorine and Hydrazine as a Rocket Motor Propellant Combination. Rep. No. AL-582, North American Aviation, Inc., July 14, 1949.

13. Terlizzi, P. M., and Klein, E. L.: Liquid Rocket Propellants. Part I - Diborane. Power Plant Memo. No. 21, Navy Dept., Bur. Aero., Aug. 1947.

14. Kiehl, S. J., Jr., and Moore, J. R.: Propellants for Supersonic Vehicles: Liquid Fluorine. Rep. No. RA-15047, Battelle Mem. Inst., August 18, 1947. (Subcontract with Douglas Aircraft Co., Inc., under AAF Contract No. W33-038-ac-14105, Project RAND.)

15. Newkirk, A. E.: Critical Temperature and Pressure of Diborane. Rep. No. 55221, Res. Lab., Gen. Elec, Co., Sept. 17, 1947. (Proj. Hermes, TU1-2000, U. S. Army Ordnance.)

16. Anon.: Tables of Selected Values of Chemical Thermodynamic Properties. Nat. Bur. Standards, Sept. 30, 1949.

2293

17. Laubengayer, A. W., Ferguson, R. P., and Newkirk, A. E.: The
    Densities, Surface Tensions and Parachors of Diborane, Boron
    Triethyl and Boron Tribromide. The Atomic Parachor of Boron.
    Jour. Am. Chem. Soc., vol. 63, no. 2, Feb. 1941, pp. 559-561.

TABLE I - PHYSICAL CONSTANTS

Constant	Fluorine, F_2	Refer-ence	Diborane, B_2H_6	Refer-ence
Boiling point, °C Pressure (atm)		--		
1	-188(-305° F)	12	-92.5(-134.5° F)	13
14.6	-154(-245° F)	12		
28.2	-141.1(-222° F)	12		
Melting point, °C	-218(-360° F)	14	-165.5(-266° F)	13
Density, g/cc Temperature (°C)				
-196	1.558[a]	--	------	--
-72			0.407[b]	
Critical tempera-ture, °C	-129(-200° F)	14	16.7(62.1° F)	15
Critical pressure, atm	55	14	40	15
Heat of formation of liquid at boiling point from elements at 25° C, kcal/mole	-3.030	5	2.7	10
Heat of vaporization, kcal/mole	1.51	5	3.45	16
Heat of fusion, kcal/mole	0.372	5	1.06	16
Specific heat, cal/°C mole	7.522	10	13.48	16
Vapor pressure, atm Temperature (°C) (°F)				
-188 -305	1	12	---	
-183 -297.4	1.4	12	---	
-196 -321	0.31	12	---	
-70 -94			2	13

[a]Unpublished value obtained at Aerojet Engineering Corp. Literature value is 1.108 at -187° C.

[b]d = 0.3140 - 0.001296 t °C (reference 17).

TABLE II - SUMMARY OF PERFORMANCE OF LIQUID DIBORANE AND LIQUID FLUORINE IN ROCKET ENGINES

Run time (sec)	Injector design	Engine characteristic length L^*	Fuel flow (lb/sec)	Oxidant flow (lb/sec)	Helium flow (lb/sec)	Total propellant flow (lb/sec)	Ratio of fuel weight to total fuel plus oxidant weight	Thrust (lb)	Experimental specific impulse (lb-sec/lb)	Chamber pressure (lb/sq in. abs.)	Total heat rejection (Btu/sec)	Experimental specific impulse, corrected (lb-sec/lb)	Experimental characteristic velocity C^* (ft/sec)	Experimental thrust coefficient C_F	Experimental volume specific impulse $\left(\dfrac{\text{lb-sec}}{\text{cu ft}} \times \dfrac{1}{32.4}\right)$
2	Modified impinging jet	60	0.0691	0.1485	------	0.2176	0.3176	32.936	151.36	105	(a)	188.43[b]	3729	1.307	125.42
6	Modified impinging jet	50	.00837	.1049	------	.11327	.0739	16.868	168.53	90	(a)	209.45[b]	6139	.8736	219.07
4	Modified impinging jet	50	.00895	.7014	------	.71035	.0126	34.336	48.33	130	(a)	76.36[b]	1414	1.101	74.59
2	Hollow-cone spray	100	.0641	.281	------	.3451	.1857	99.000	286.87	271	(a)	302.00[b]	6069	1.522	297.21
2	Shower head	50	.1015	.2578	------	.3593	.2826	69.729	194.07	200	(a)	214.74[b]	4302	1.455	169.86
7	Four-one-helium	50	.1323	.3635	0.0110	.5068	.2682	85.712	169.12	310	87.73	175.51	4727	1.152	151.84
5	Four-one-helium	100	.0377	.334	.0152	.3869	.1014	106.26	274.64	340	>120.32	276.77	6791	1.302	338.77
13	Four-one-helium	100	.0458	.2821	.0152	.3431	.1397	100.38	292.57	283	>155.84	302.43	6574	1.478	332.13
17	Four-one-helium	100	.0664	.2899	.0152	.3715	.1864	89.880	241.94	300	127.12	251.34	6241	1.248	250.33
12	Four-one-helium	50	.0555	.3400	.0145	.4100	.1403	79.924	194.94	266	146.45	208.12	5014	1.252	221.02
14	Four-one-helium	88.8	.0554	.3344	.0100	.3998	.1421	92.906	232.38	289	298.84	250.10	6356	1.186	262.49
15	Four-one-helium	100	.0663	.2915	.0070	.3648	.1853	80.201	219.85	281	218.92	239.44	5953	1.189	227.94
14	Four-one-helium	100	.0556	.3376	.0047	.3979	.1370	109.50	275.26	311	324.99	289.17	6042	1.467	314.22
16	Four-one-helium	100	.0543	.3059	.0072	.3674	.1507	94.770	257.95	311	260.96	271.95	6542	1.270	286.26
20	Four-one-helium	100	.0617	.2572	.0072	.3261	.1935	85.654	262.66	287	241.15	283.07	6801	1.244	268.16
7	Four (two-one-helium)	100	.0541	.3188	.0116	.3845	.1451	103.44	289.02	305	150.00	276.35	6130	1.413	302.00
4	Four-one-helium	50	.0575	.2868	.0072	.3515	.1670	95.675	272.19	287	171.59	284.07	6310	1.389	292.39
5	Four-one-helium	50	.0364	.4580	.0072	.5016	.0756	100.26	199.92	322	158.26	209.32	4961	1.298	263.12
7	Four-one-helium	100	.0795	.3306	.0072	.4173	.1939	114.35	274.02	338	275.40	286.94	6260	1.410	279.56
7	Four-one-helium	100	.0411	.3705	.0072	.4188	.0999	106.85	285.13	314	200.20	263.38	5794	1.418	315.72

[a] Engine burnout.
[b] Correction based on estimated heat rejection.

NACA
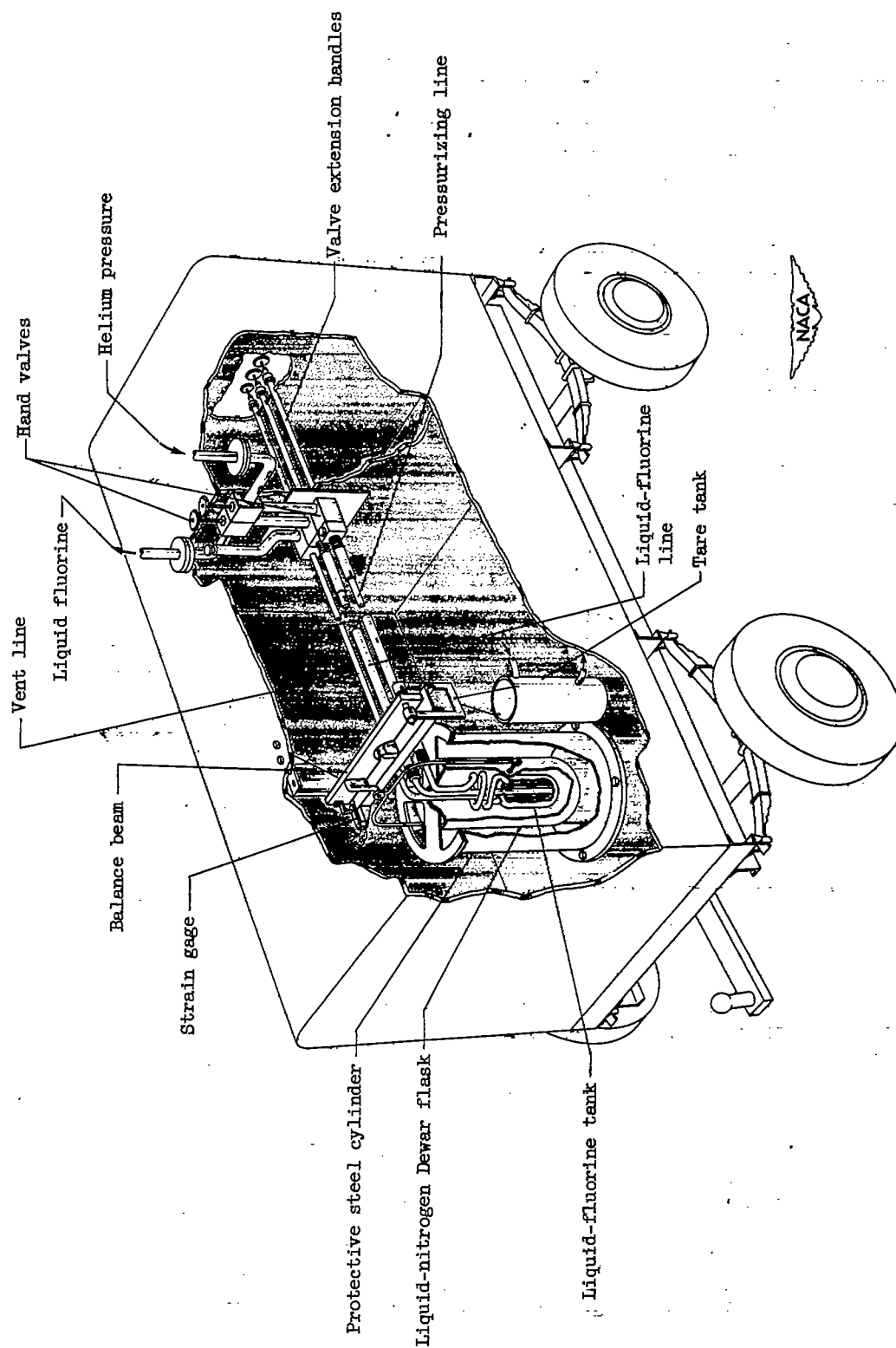
Figure 1. - Liquid-fluorine trailer.

Fluorine flow tube

Pressurizing line

Vent

Nitrogen tank cover

Liquid
nitrogen
tank

Nitrogen
tank float
and rod

Liquid
fluorine
tank

Pneumatic
cylinder

Liquid
fluorine

Liquid
nitrogen

NACA
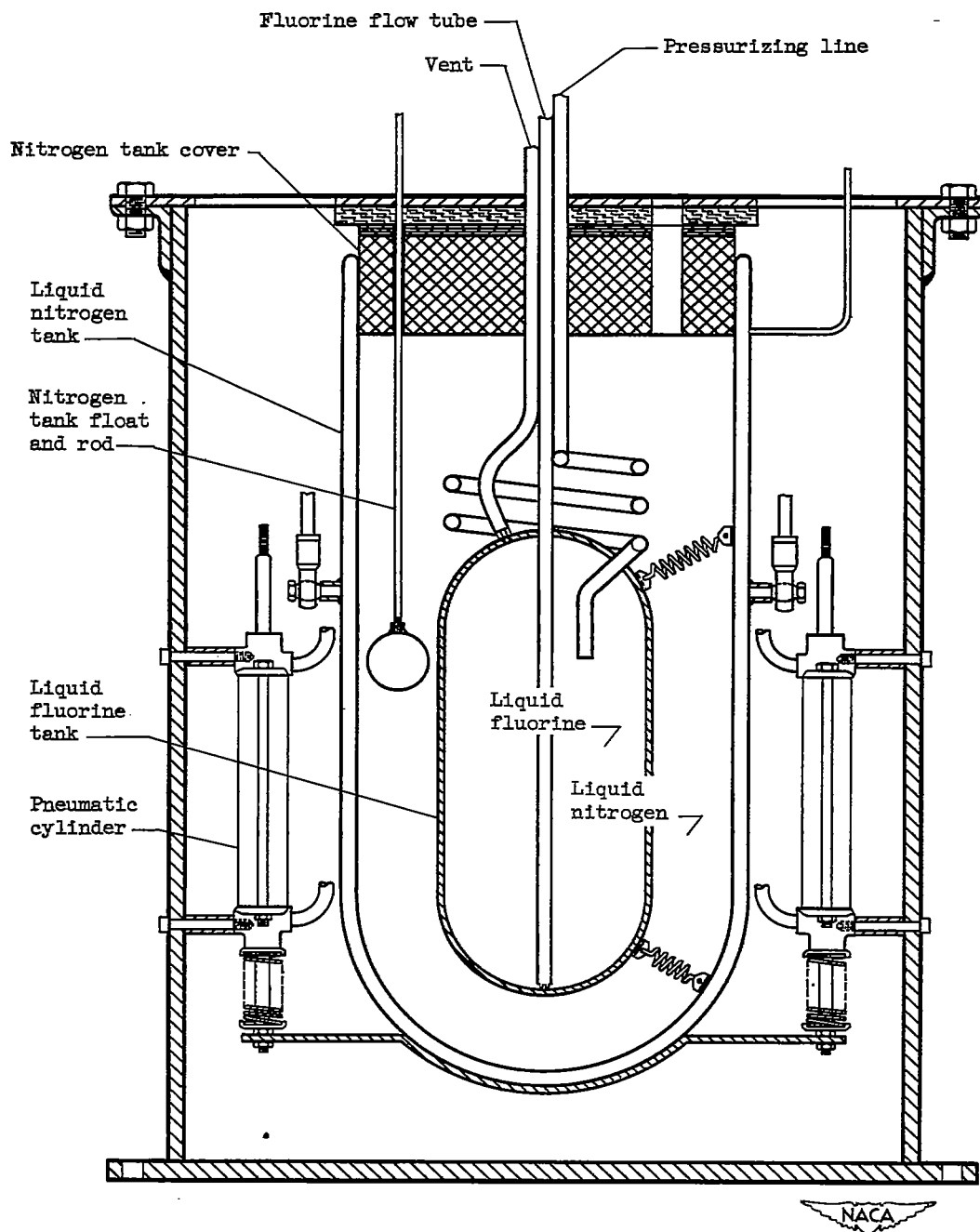
Figure 2. - Liquid-fluorine tank assembly.

Balance beam

Diborane supply tank

Diborane tank

Water pump for cooling injector

Rocket engine

Flow meter

Water tank

Vacuum pump

Steel barrier

Fluorine-supply cylinder

Nitrogen tank

Nitrogen cylinders

Fluorine tank

Liquid-nitrogen Dewar flask

Helium cooler

Precooling nitrogen tank

Filter

Helium cylinders

Remote operating valve

Pressure regulator

Pressure regulator

Fluorine
Diborane
Helium (gas)
Vacuum
Water
Nitrogen (liquid)
Nitrogen (gas)

Figure 3. - Diagrammatic sketch of 100-pound-thrust rocket apparatus for investigation of liquid fluorine and liquid diborane.
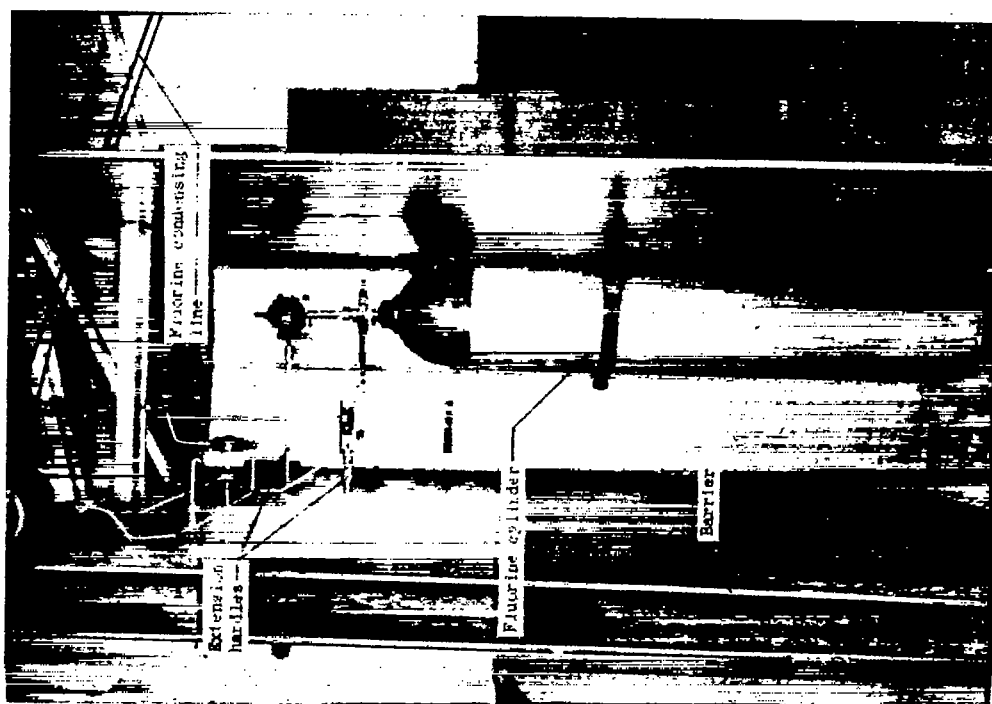
(a) Fluorine supply cylinder in protective barrier.
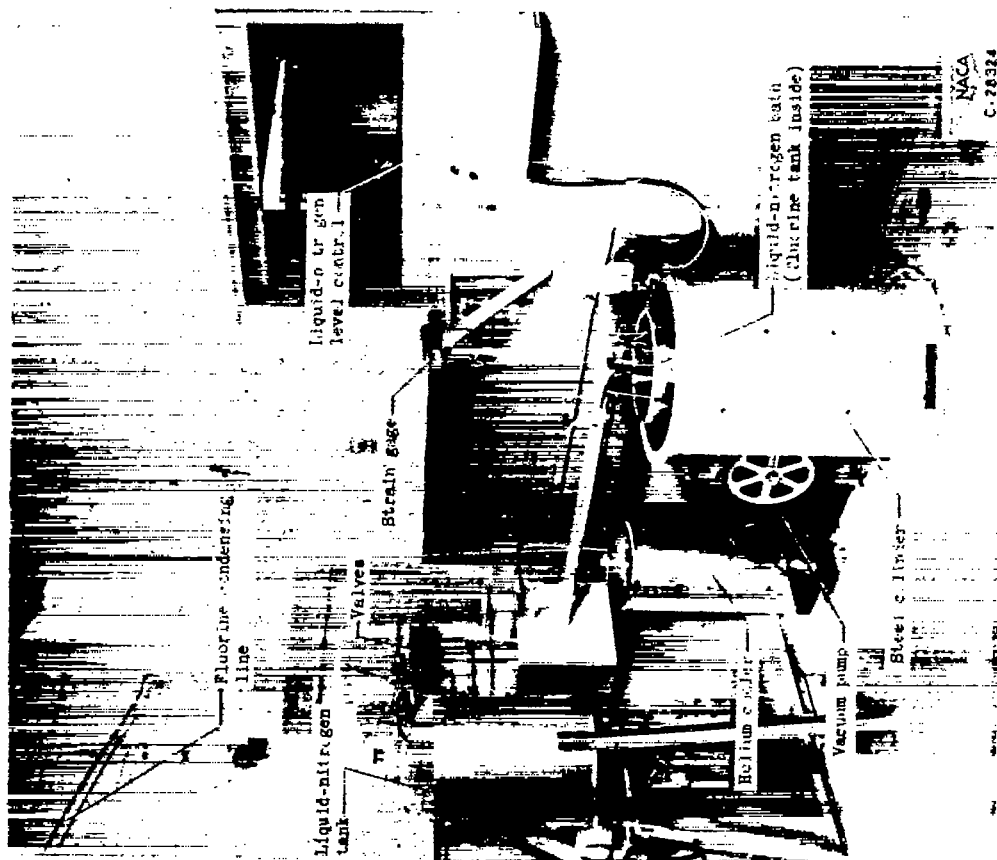
(b) Liquid-fluorine tank in liquid-nitrogen bath and related equipment.

Figure 4. - Fluorine propellant handling system.
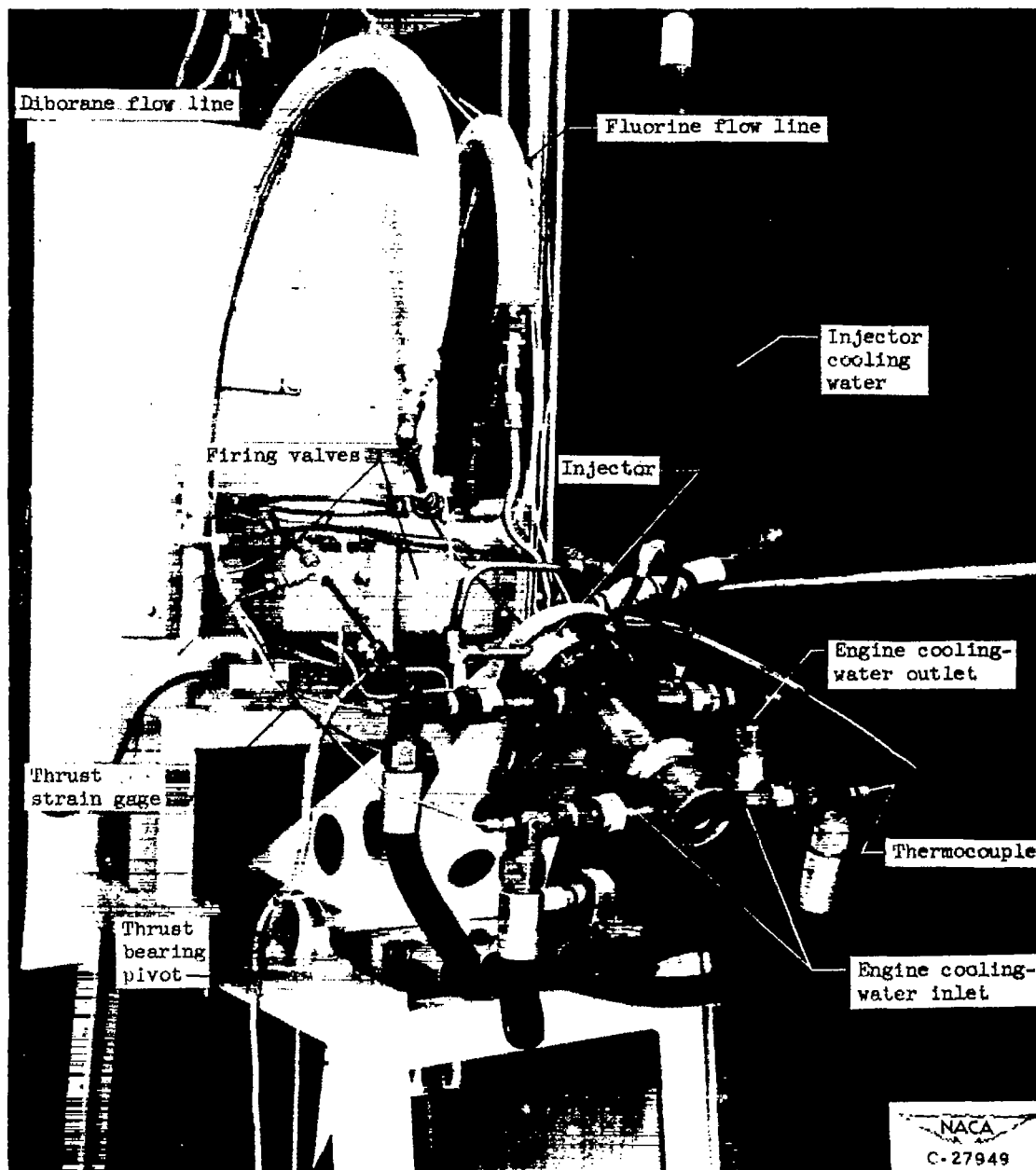
Figure 5. - Rocket engine mounted on thrust stand.
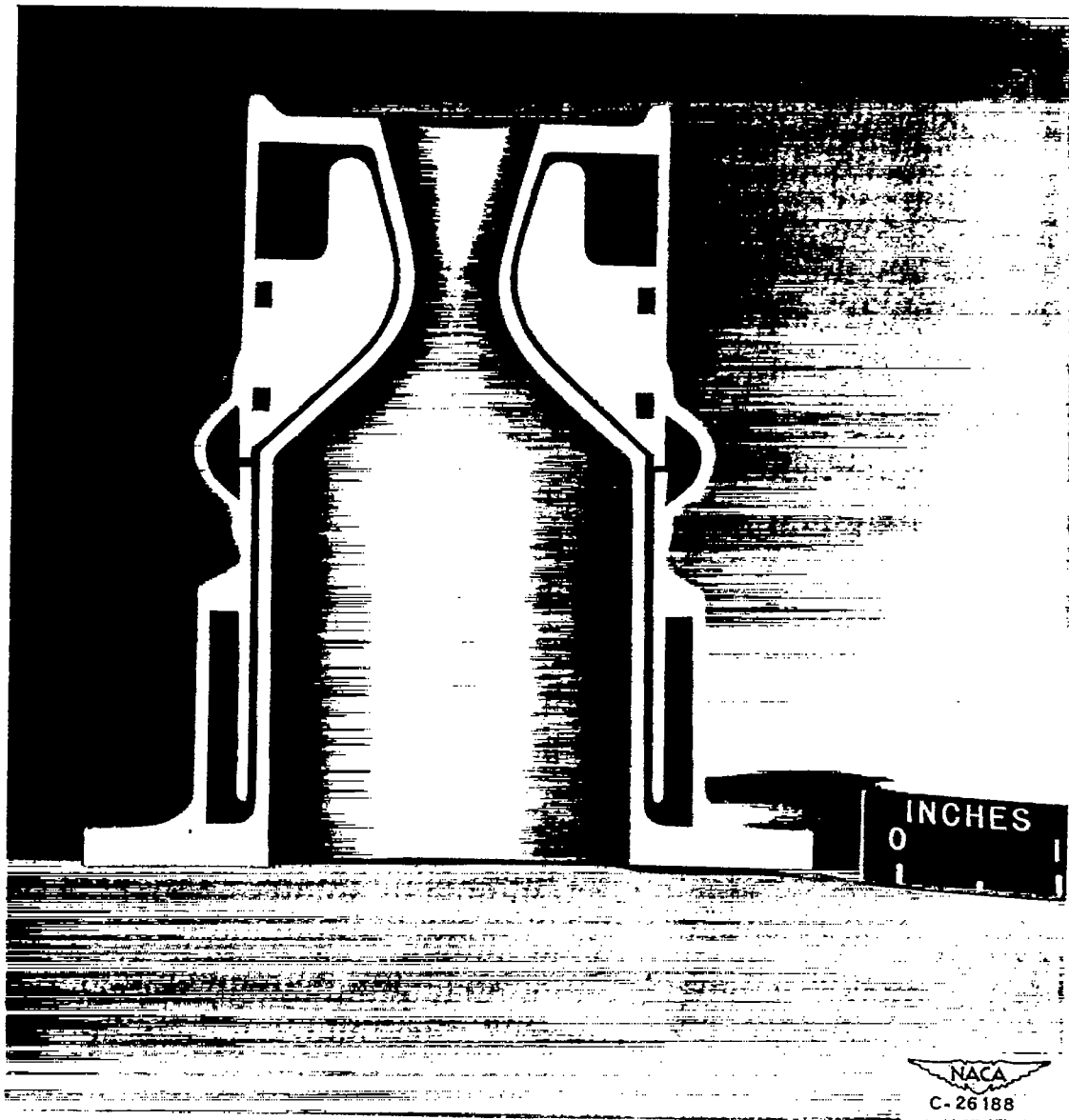
Figure 6. – Section through chamber and nozzle of 50 L* engine.
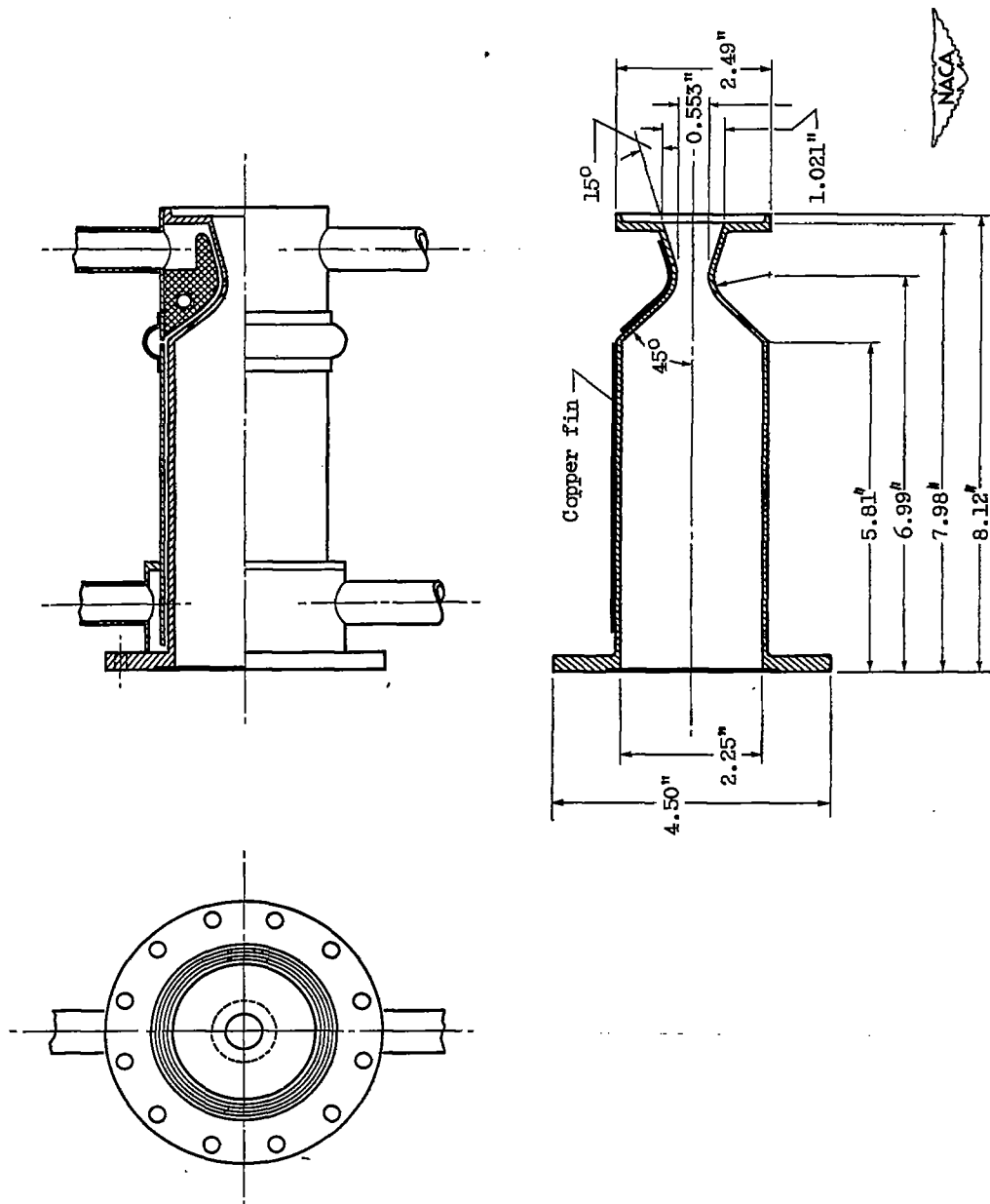
Figure 7. - Combustion chamber and nozzle of 100 L* engine.
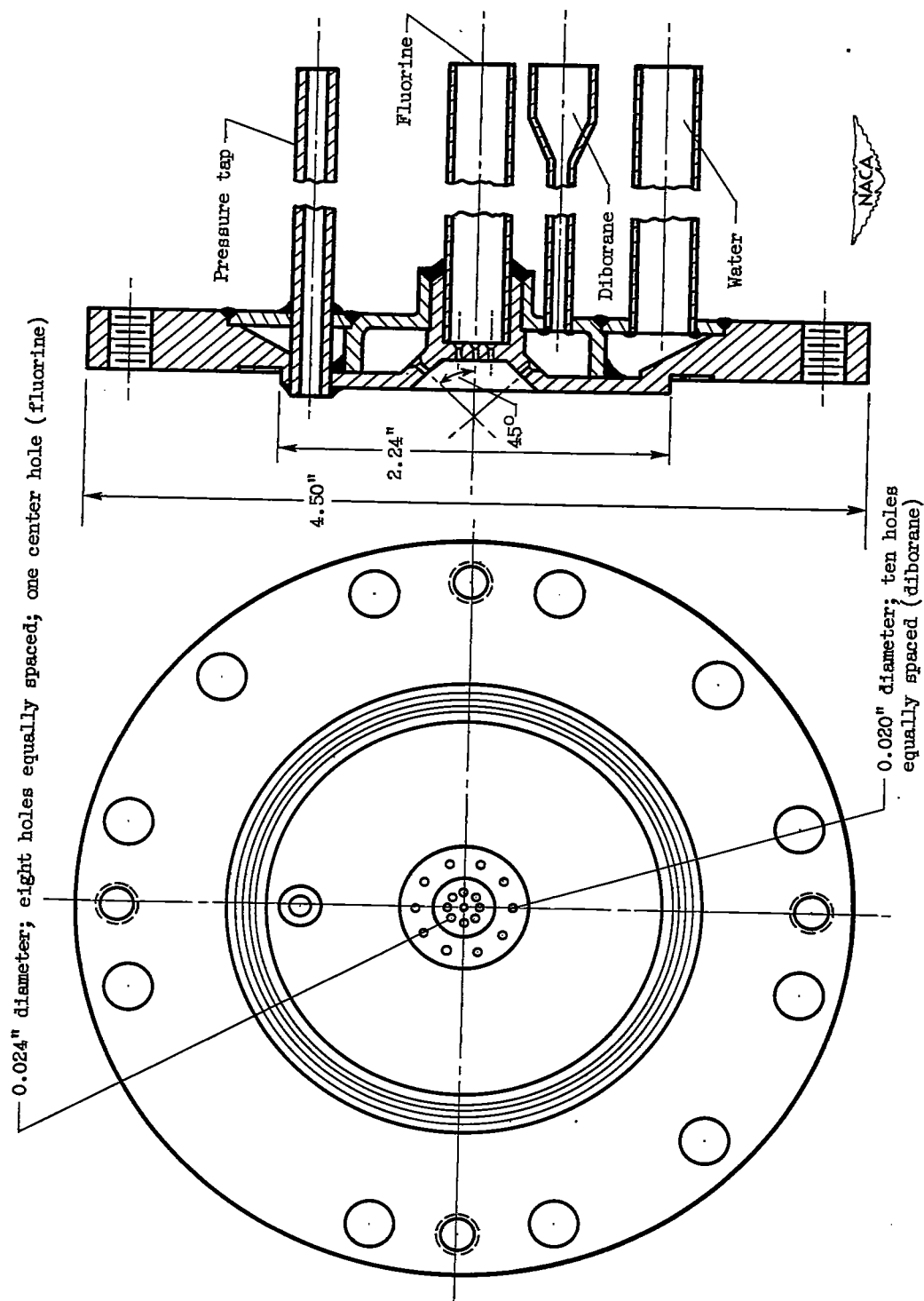
Figure 8. – Modified multiple impinging-jet injector.

0.065" diameter;
one hole

Pressure tap

Fluorine

4.50"

2.24"

30°

Diborane

Water

0.058" diameter;
four holes equally
spaced

30°

0.16"

0.50"

NACA
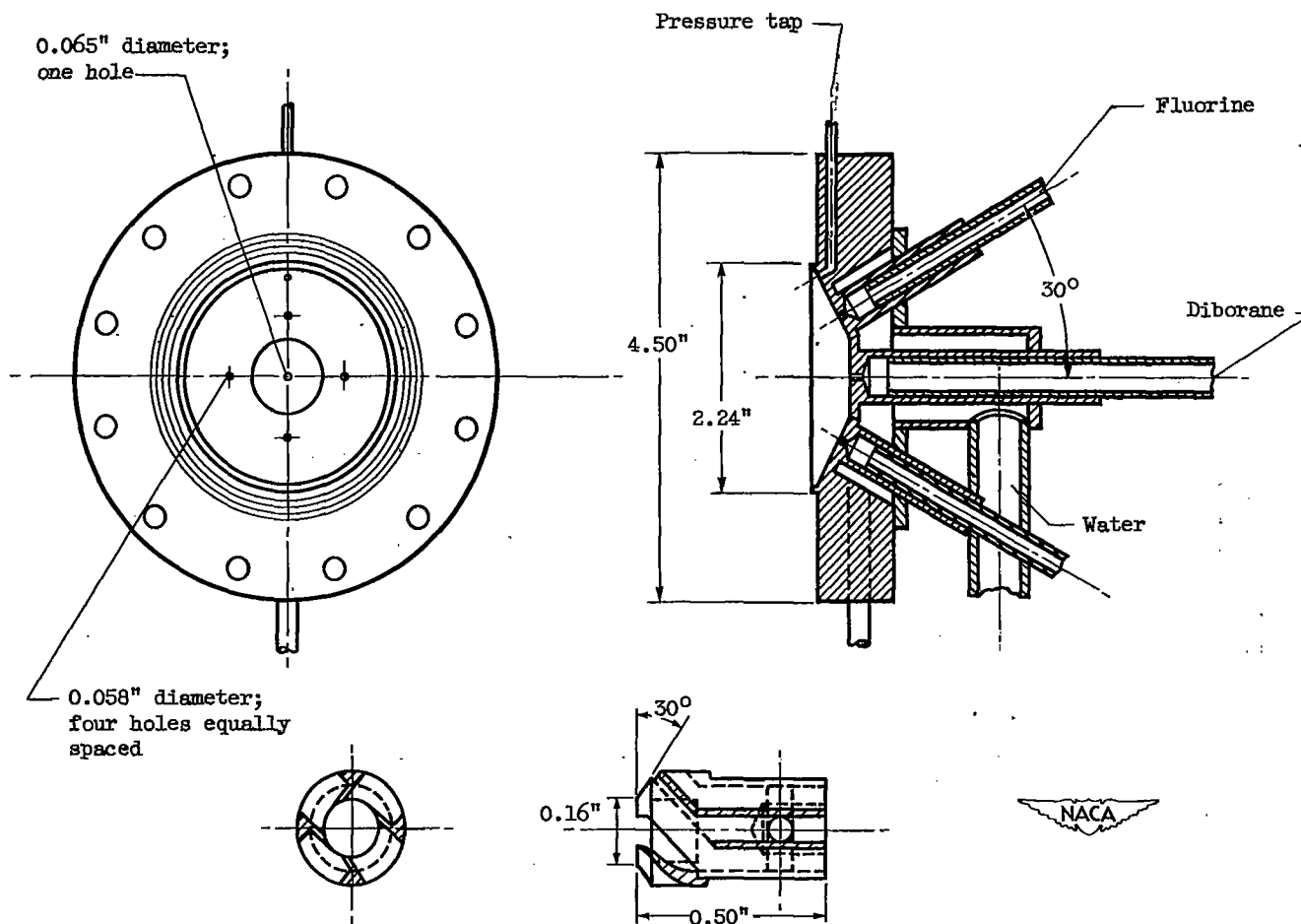
Figure 9. - Hollow-cone spray type injector.
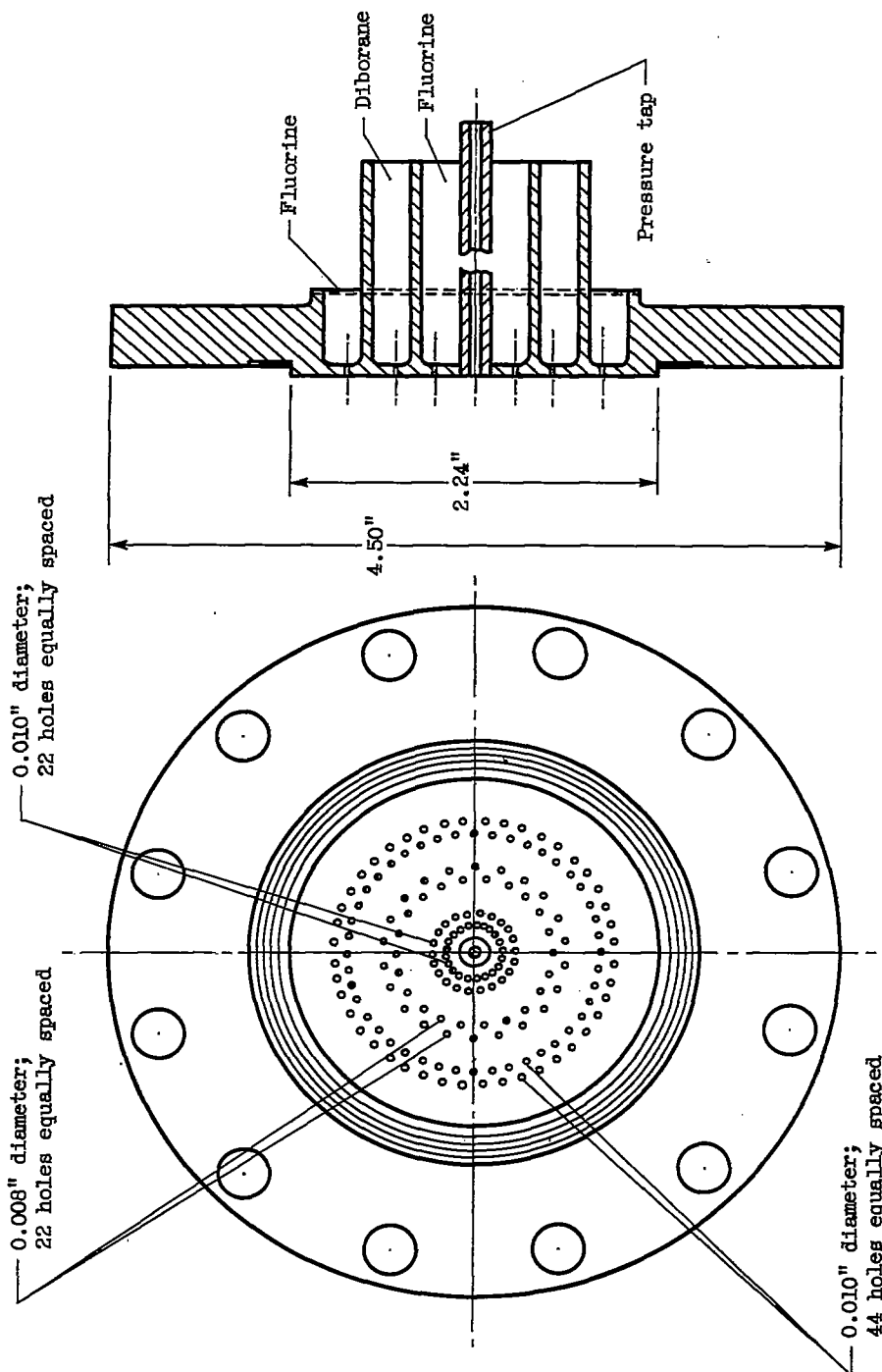
Figure 10. – Shower-head injector.

Fluorine

Water

Diborane

0.125 O.D. × 0.031
wall tubing

Helium

30°

2.24"

4.50"

0.063" diameter

0.020" annulus

0.060" diameter;
four holes equally spaced

NACA
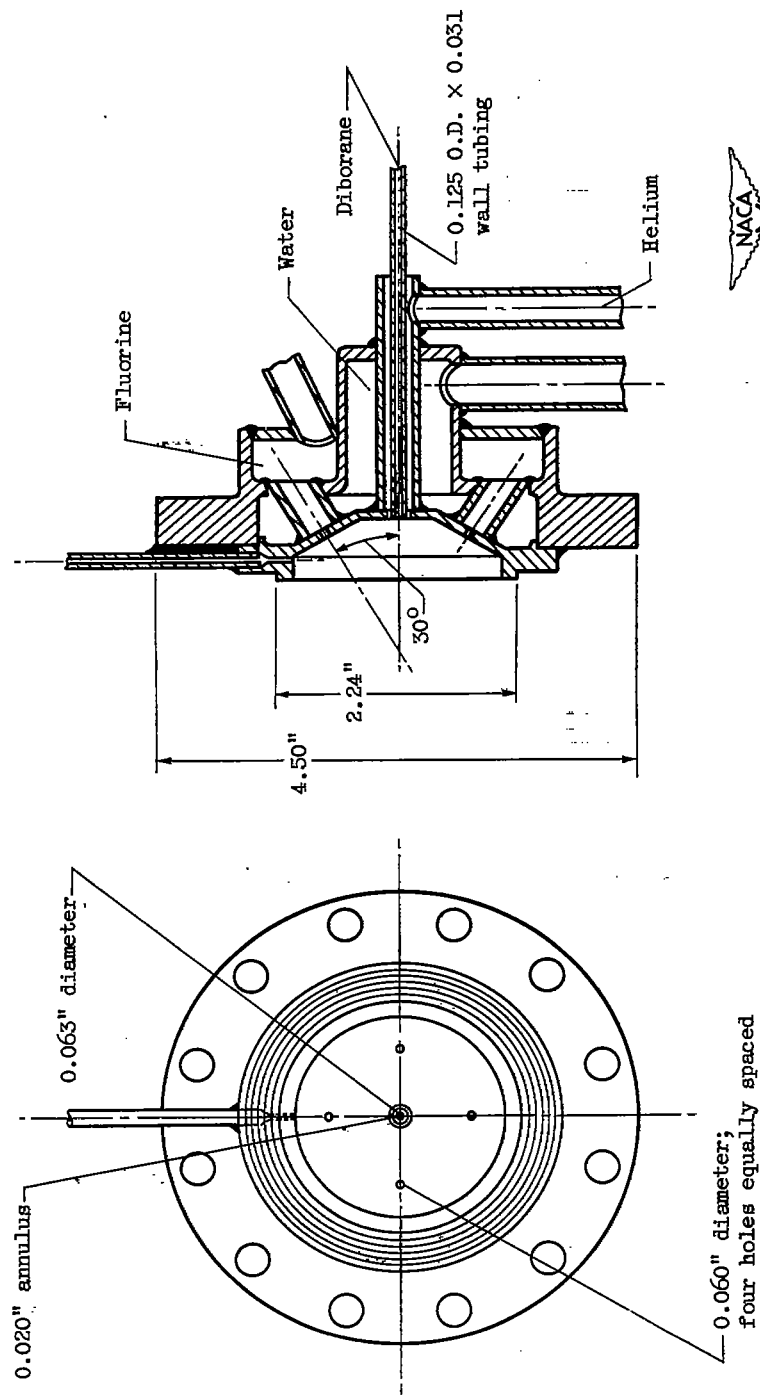
Figure 11. - Four fluorine - one diborane, helium protected, impinging-jet injector.

0.004 annulus and 0.032 diameter;
four sets equally spaced

0.062" O.D. × 0.015"
wall tubing

Fluorine

Helium

4.50"

45°

2.24"
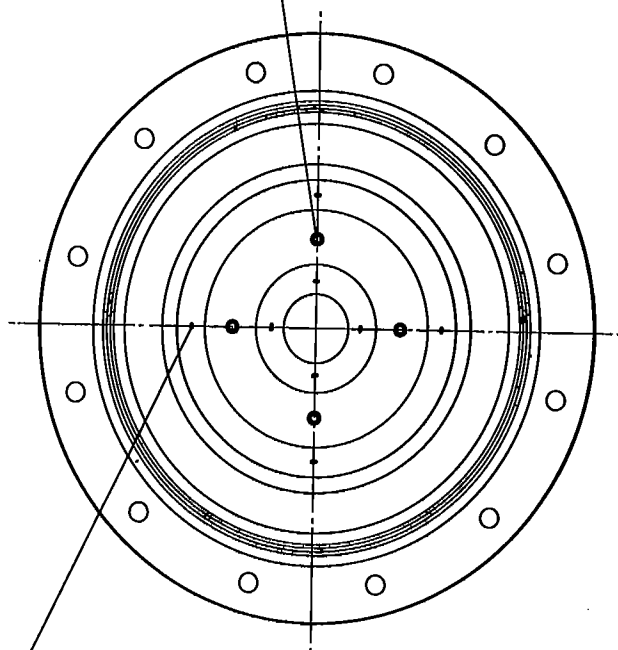
Diborane

Fluorine

0.033" diameter; two rows four
holes each equally spaced

NACA
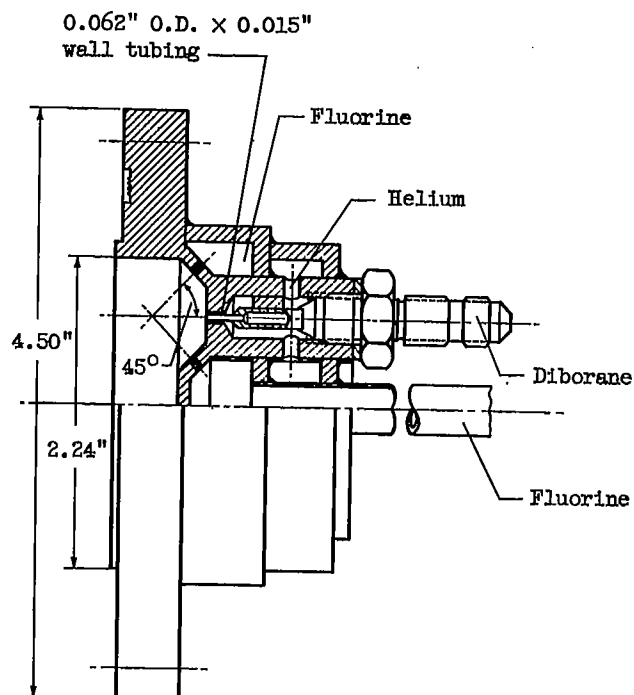
Figure 12. - Four unit two fluorine - one diborane, helium protected, impinging-jet injector.
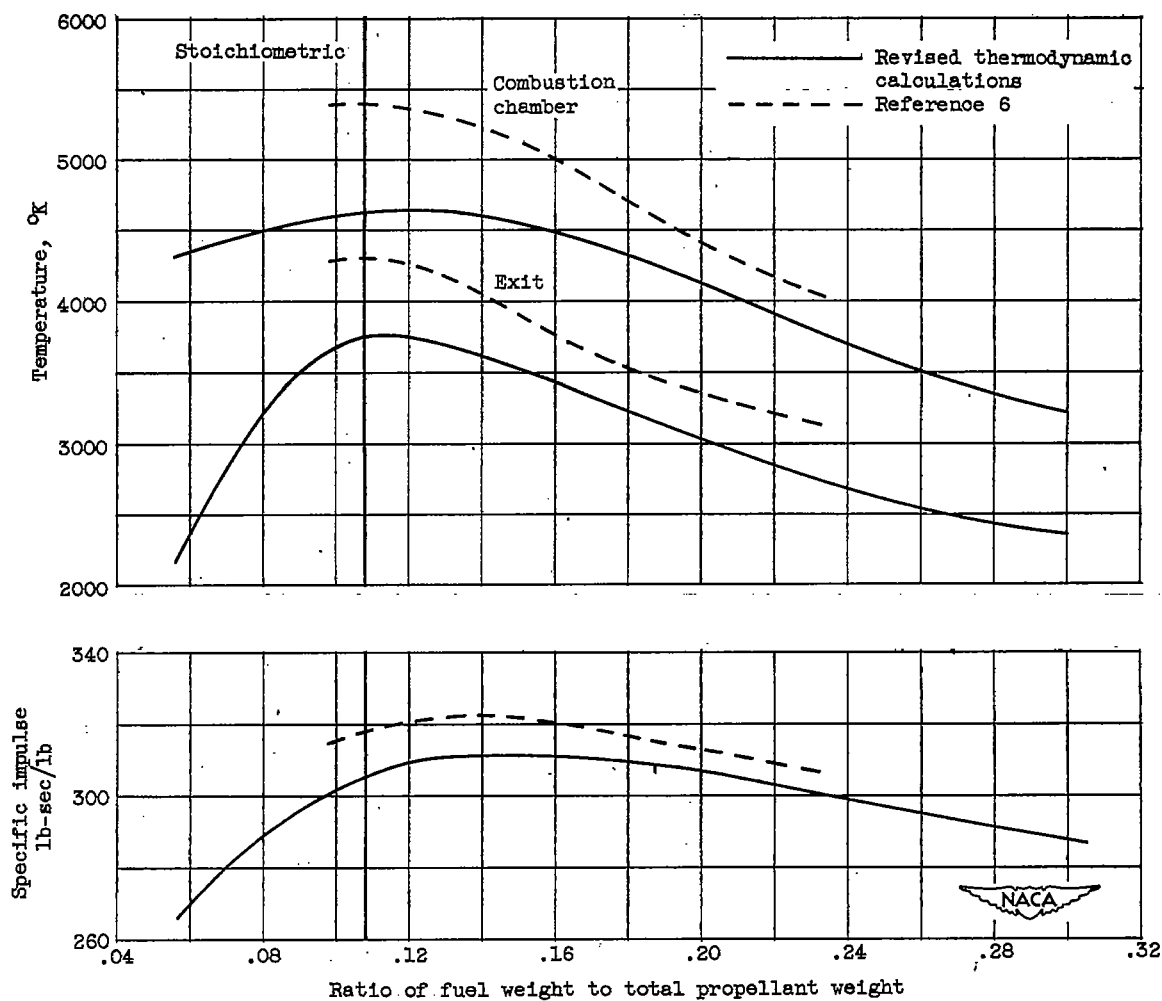
Figure 13. - Theoretical performance of liquid fluorine - liquid diborane propellant combination.
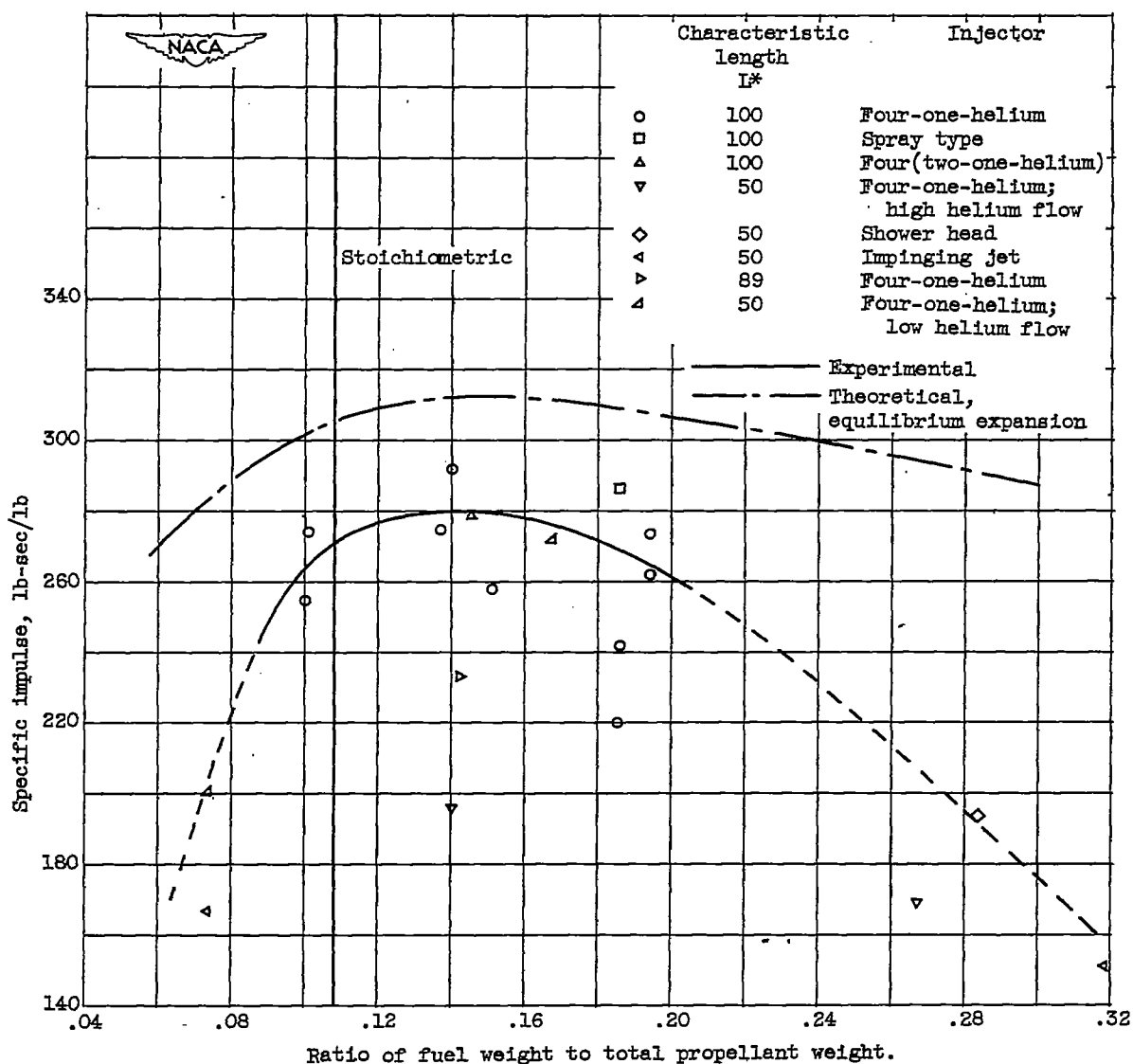
(a) Comparison of measured and calculated values.

Figure 14. - Theoretical and experimental specific impulse of liquid fluorine and liquid diborane in 100-pound-thrust rocket engine.
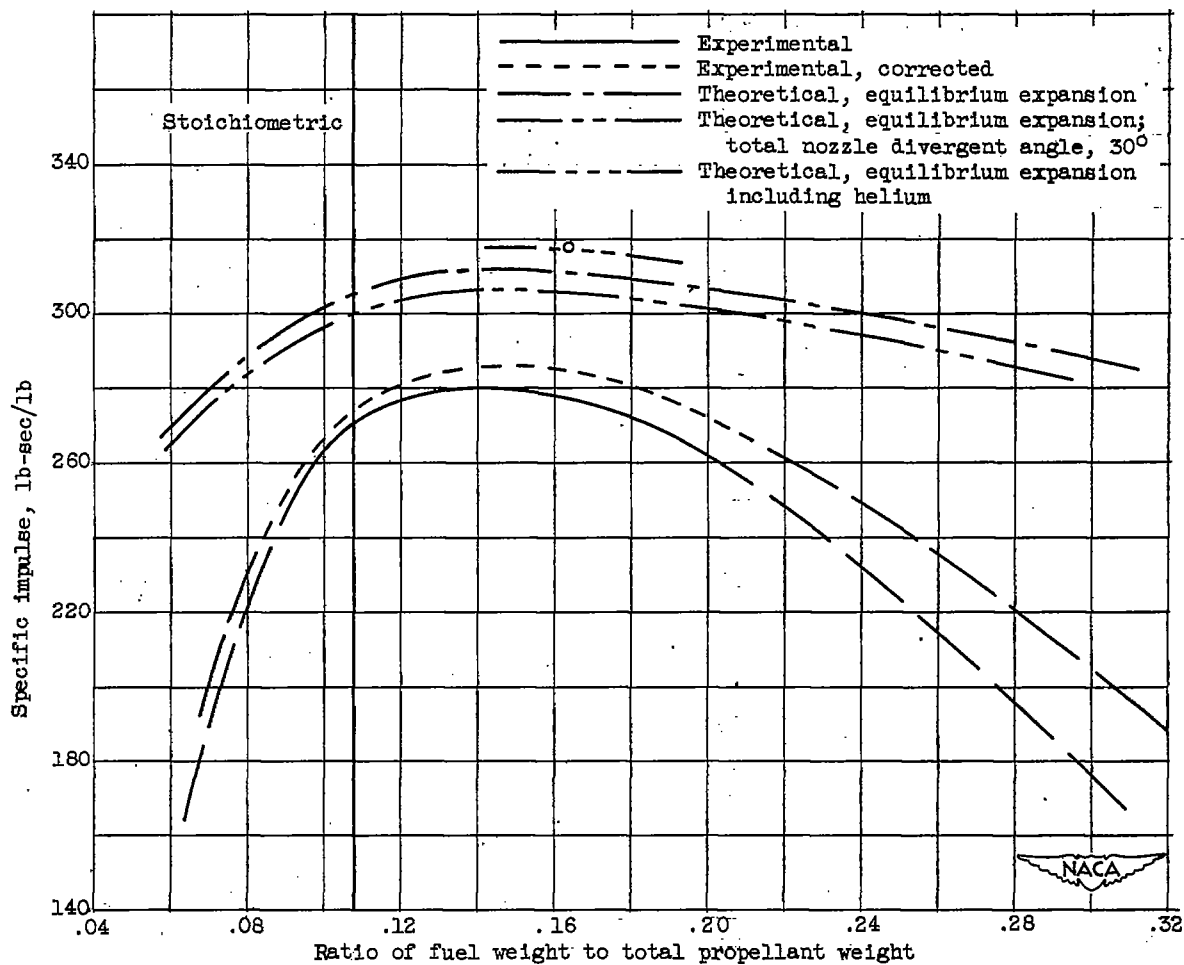
(b) Comparison of measured, calculated, and corrected values.

Figure 14. - Concluded. Theoretical and experimental specific impulse of liquid fluorine and liquid diborane in 100-pound-thrust rocket engine.
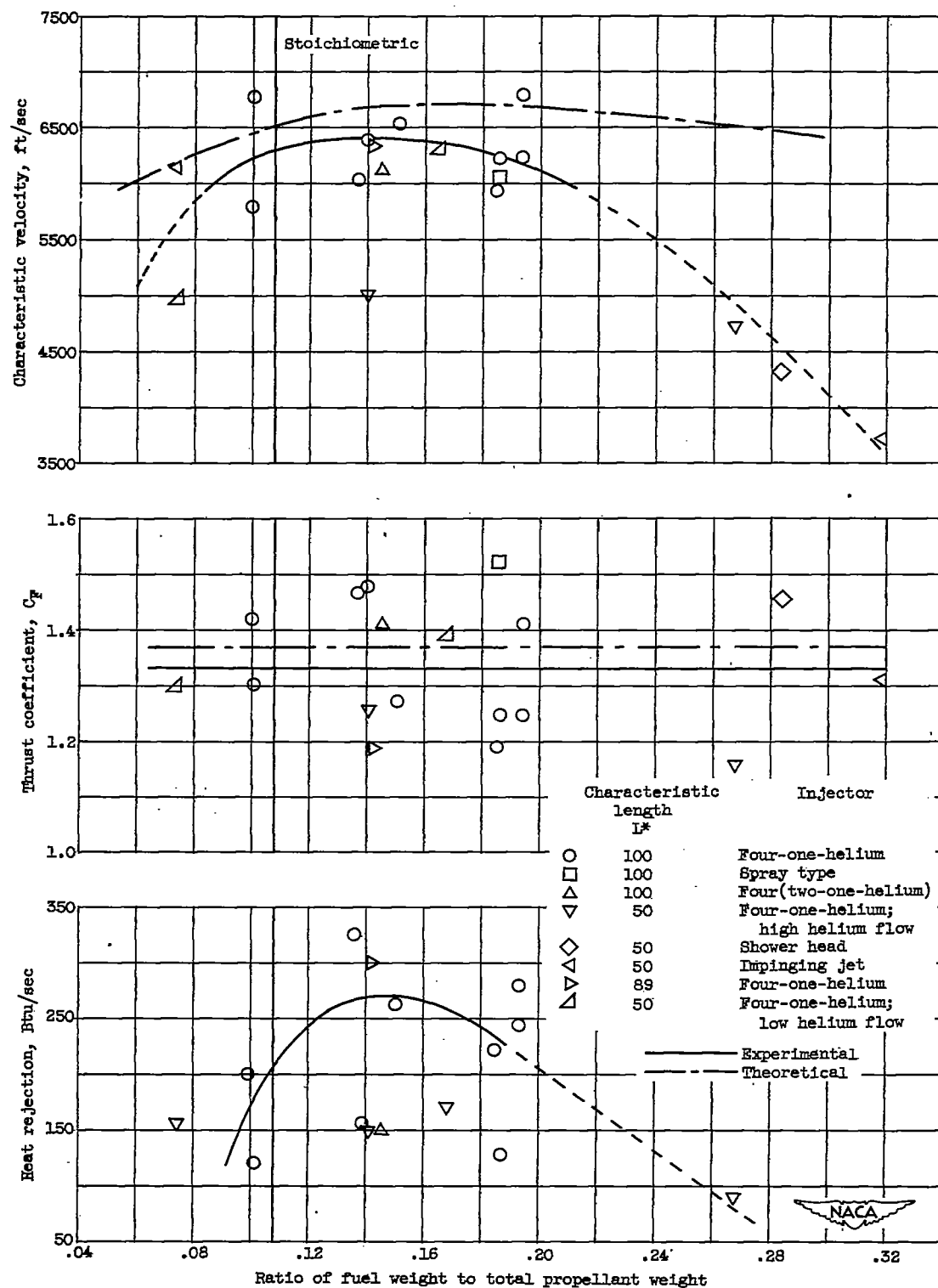
2293

Stoichiometric

Characteristic velocity, ft/sec

7500

6500

5500

4500

3500

Thrust coefficient, C_F

1.6

1.4

1.2

1.0

	Characteristic length L^*	Injector
O	100	Four-one-helium
□	100	Spray type
△	100	Four(two-one-helium)
▽	50	Four-one-helium; high helium flow
◇	50	Shower head
◁	50	Impinging jet
▷	89	Four-one-helium
◿	50	Four-one-helium; low helium flow

———— Experimental
—·—·— Theoretical

Heat rejection, Btu/sec

350

250

150

50

.04 .08 .12 .16 .20 .24 .28 .32

Ratio of fuel weight to total propellant weight

Figure 15. - Characteristic velocity, thrust coefficient, and heat rejection of liquid fluorine and liquid diborane in 100-pound-thrust rocket engine.
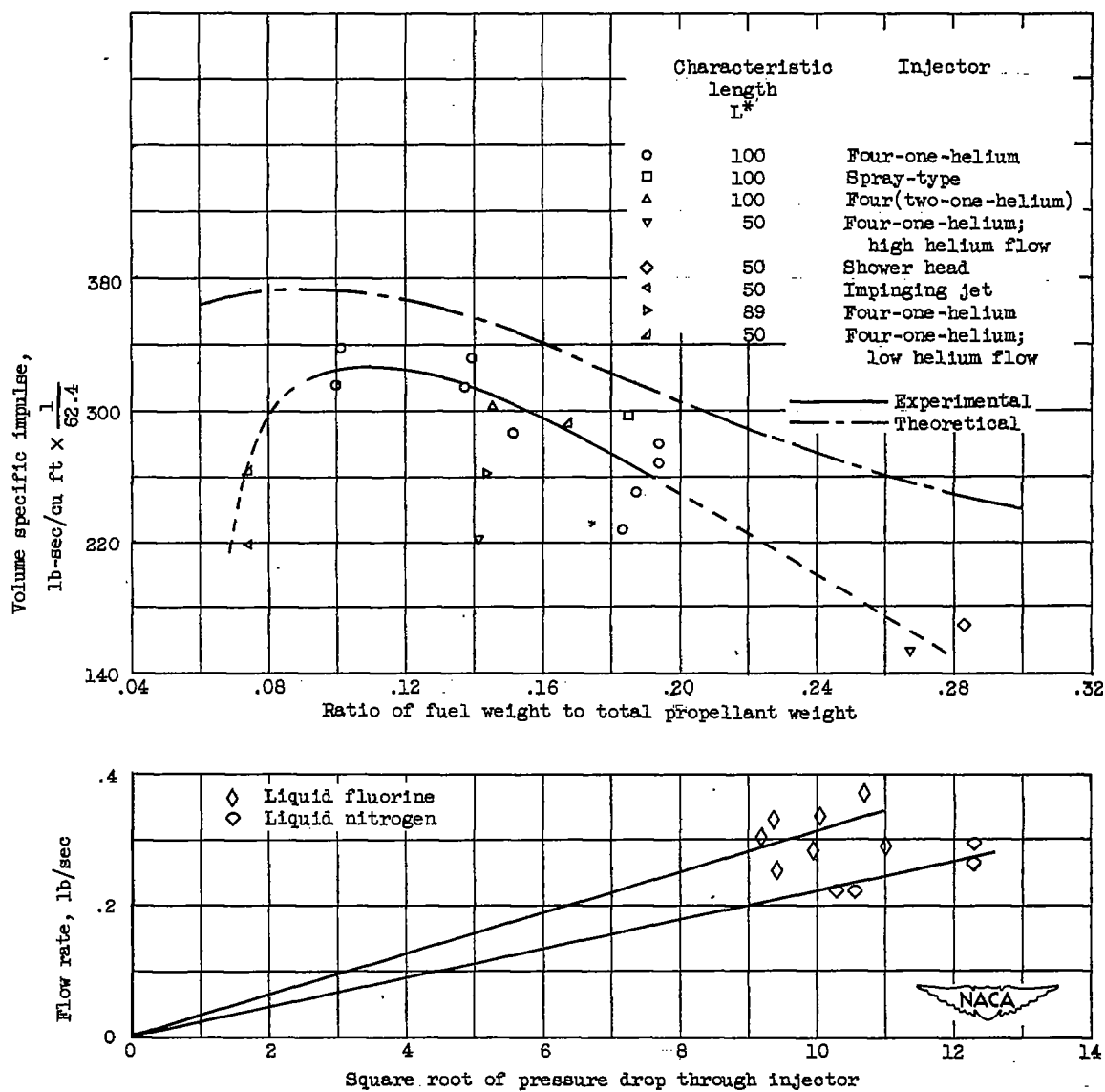
Figure 16. - Volume specific impulse of liquid fluorine and liquid diborane in 100-pound-thrust engine and flow rate of liquids through injector.
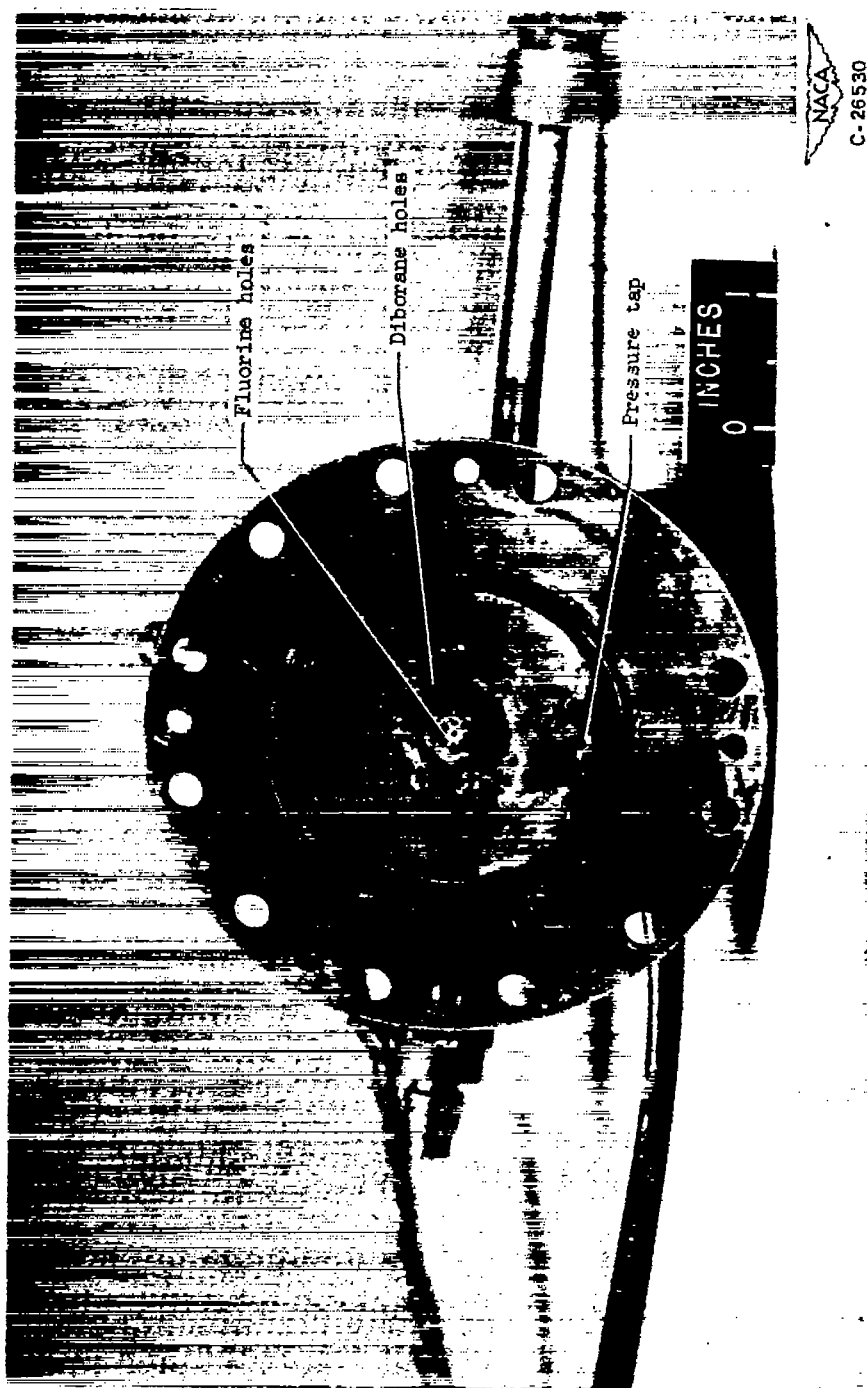
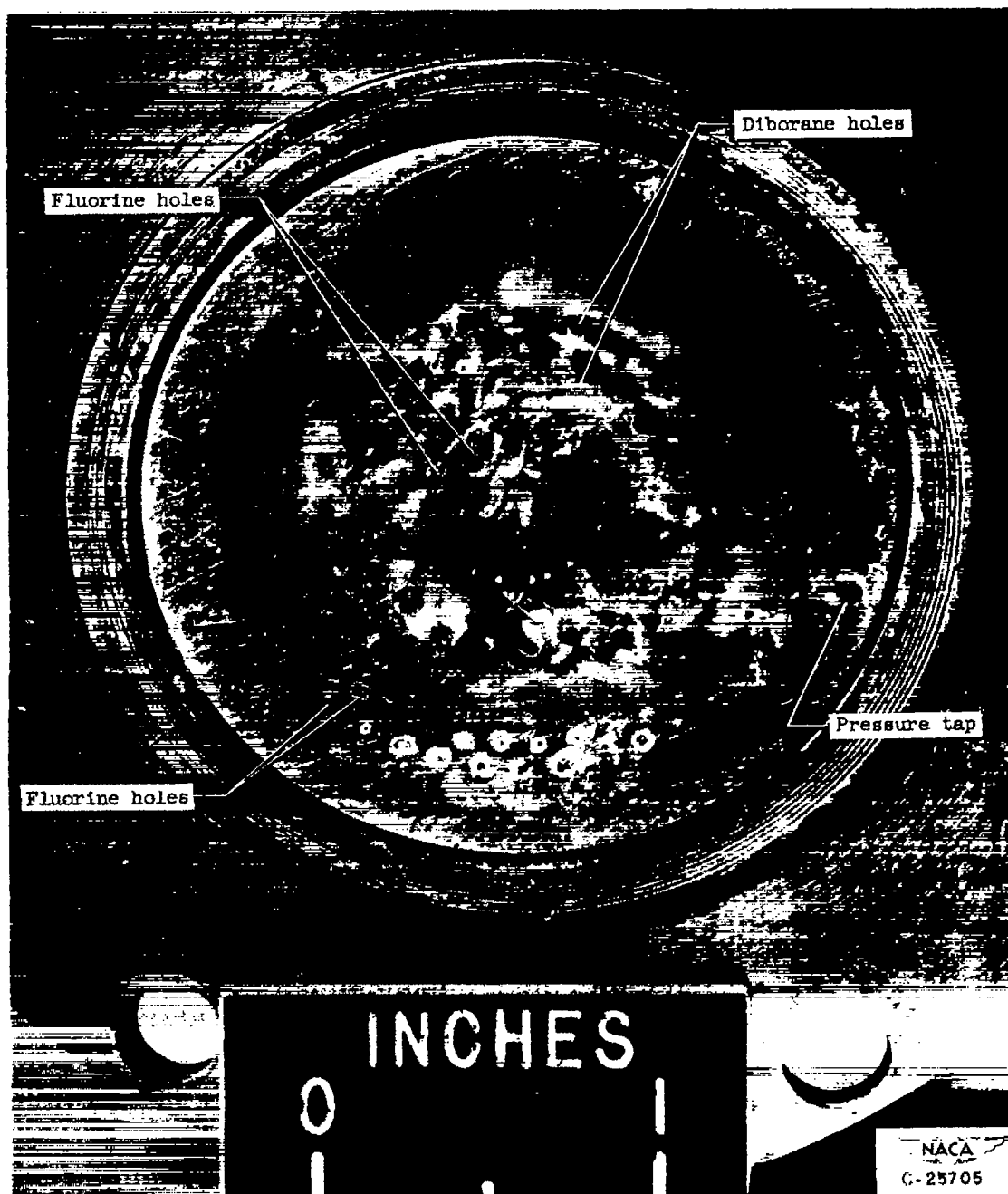Figure 17. – Burnout of diborane holes of modified multiple impinging-jet injector.

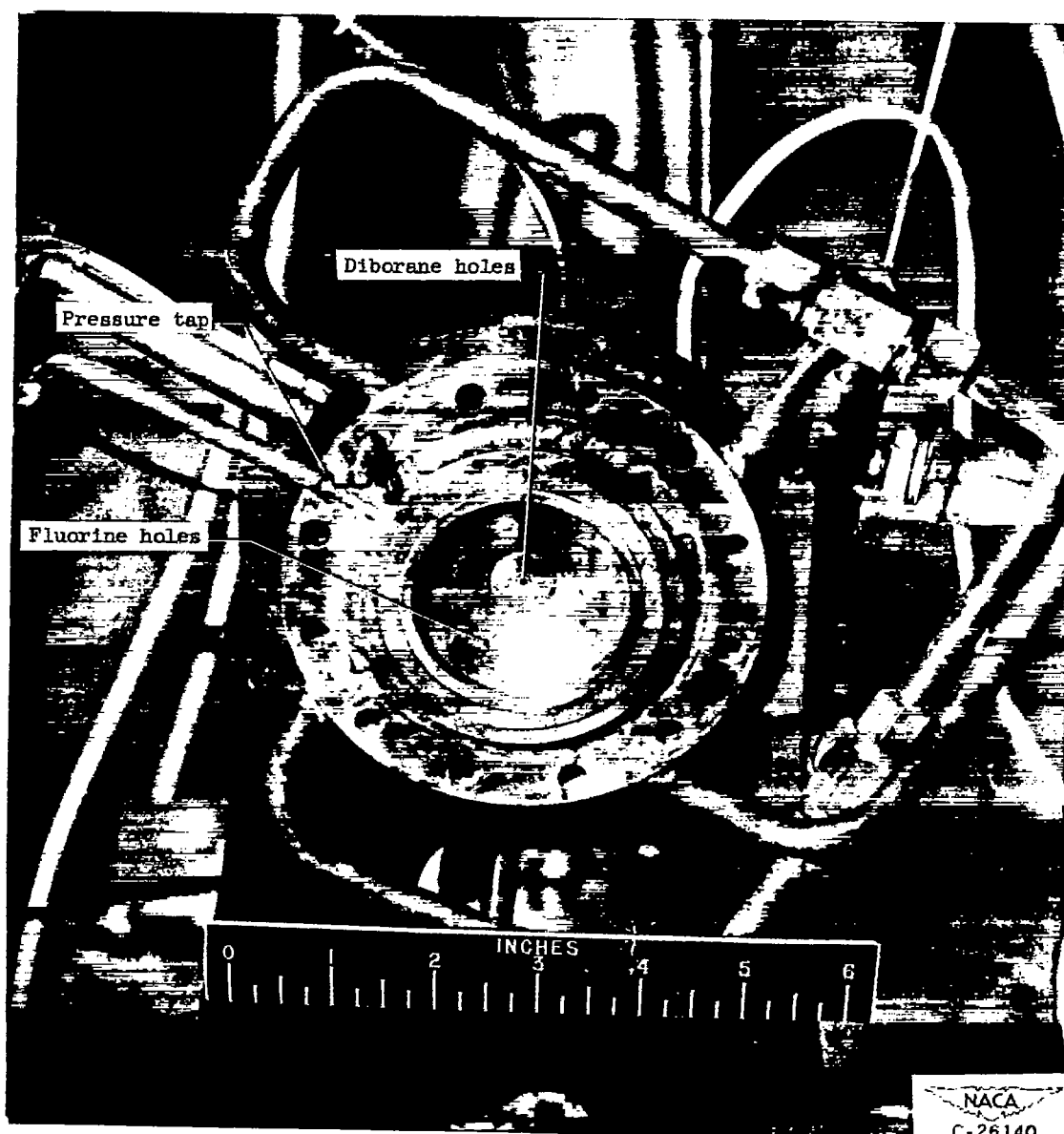Figure 18. - Welded diborane holes of shower-head injector.

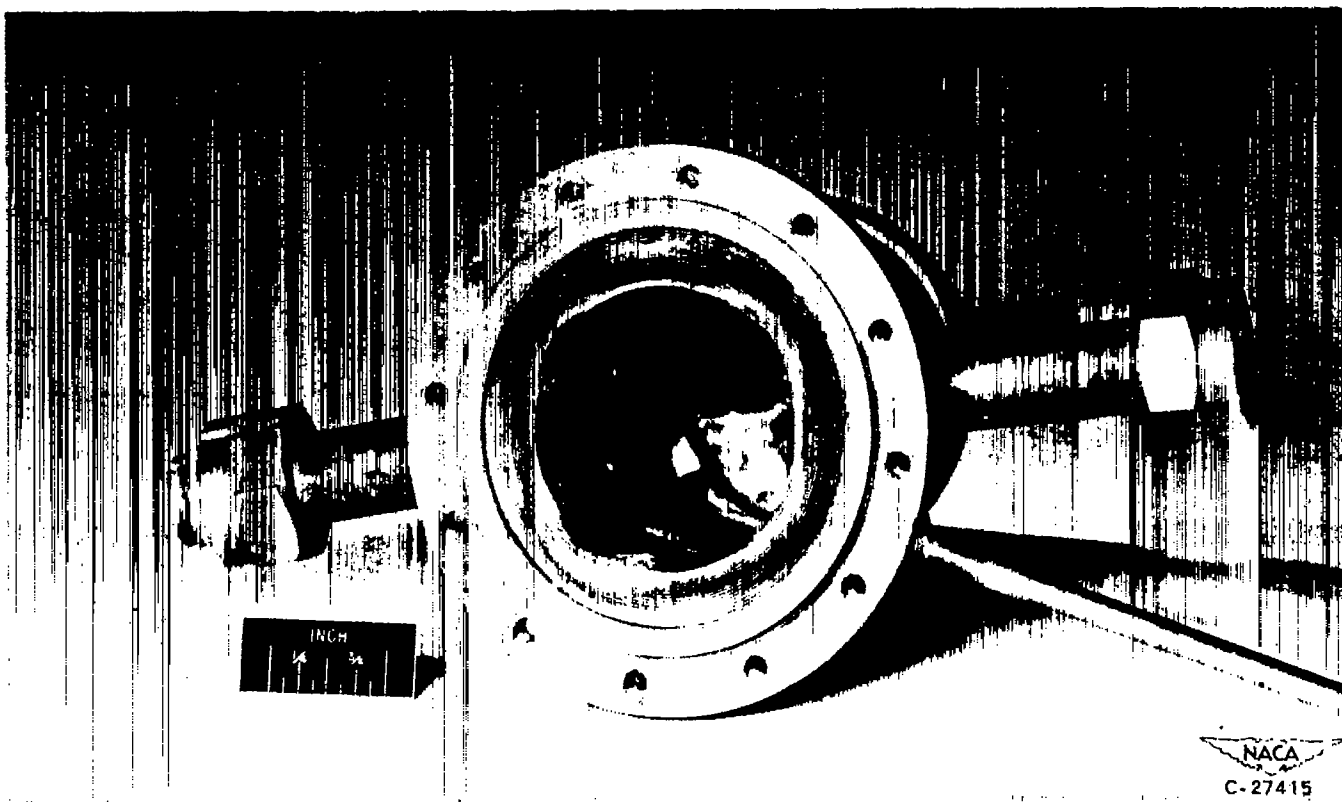Figure 19. - Four fluorine - one diborane, helium protected, impinging-jet injector after run.

Figure 20. - Pattern of burning at engine flange using four-one, helium-protected, impinging-jet injector.